

## **2.0 STRUCTURAL EVALUATION**

This section presents evaluations demonstrating that the RAJ-II package meets applicable structural criteria. The RAJ-II packaging, consisting of unirradiated fuel assemblies that provide containment, an inner container, and an outer container with paper honeycomb spacers, is evaluated and shown to provide adequate protection for the payload. Normal Conditions of Transport (NCT) and Hypothetical Accident Condition (HAC) evaluations, using analytic and empirical techniques, are performed to address 10 CFR 71 performance requirements.

Numerous tests were successfully performed on the RAJ-II package during its initial qualification in Japan that provided a basis for selecting the certification tests. RAJ-II certification testing involved two full-scale Certification Test Units (CTU) at Oak Ridge, TN. The RAJ-II CTUs were subjected to a series of free drop and puncture drop tests. The RAJ-II CTU protected the simulated fuel assemblies, allowing them to remain undamaged and leak tight throughout certification testing. Details of the certification test program are provided in Appendix 2.12.1.

### **2.1 DESCRIPTION OF STRUCTURAL DESIGN**

#### **2.1.1 Discussion**

A comprehensive discussion on the RAJ-II packaging design and configuration is provided in chapter 1.0. Drawings provided in Appendix 1.4.1 show the construction of the RAJ-II and how it protects the fuel assemblies. The containment is provided by the fuel cladding and welded end fittings of the fuel rods. The fuel is protected by an inner container that provides thermal insulations and soft foam that protects the fuel from vibration. The inner container is supported by vibration isolation system inside the outer container that has shock absorbing blocks of balsa and honeycomb made of resin impregnated kraft paper (hereinafter called "paper honeycomb"). Specific discussions relating to the aspects important to demonstrating the structural configuration and performance to design criteria for the RAJ-II packaging are provided in the following sections. Standard fabrication methods are used to fabricate the RAJ-II package.

Detailed drawings showing applicable dimensions and tolerances are provided in Appendix 1.4.1.

Weights for the various components and the assembled packaging are provided in Section 2.1.3.

##### **2.1.1.1 Containment Structures**

The primary containment for the radioactive material in the RAJ-II is the fuel rod cladding, which is manufactured to high standards for use in nuclear reactors. The fabrication standards for the fuel are in excess of what is needed to provide containment for shipping of the fuel. The fuel rod cladding is designed to provide containment throughout the life of the fuel, prior to

loading, in transportation, and while used in the reactor where it operates at higher pressures and temperatures, and must contain fission products as well as the fuel itself.

The cladding tubes for the fuel are high quality seamless tubing. The clad fuel is verified leaktight before shipment.

### **2.1.1.2 Non-Containment Vessel Structures**

The RAJ-II is made up of two non-containment structures, the inner container, and the outer container that are designed to protect the fuel assemblies and clad rods which serve as the containment. The inner container design provides some mechanical protection although its primary function is to provide thermal protection. The outer container consists of a metal wall with shock absorbing devices inside and vibration isolation mounts for the inner container. Section 1.2.1 provides a detailed description of the inner and outer container. Non-containment structures are fabricated in accordance with the drawings in Appendix 1.4.1.

Welds for the non-containment vessel walls are subjected to visual inspection as delineated on the drawings in Appendix 1.4.1.

## **2.1.2 Design Criteria**

Proof of performance for the RAJ-II package is achieved by a combination of analytic and empirical evaluations. The acceptance criteria for analytic assessments are in accordance with 10 CFR 71 and the applicable regulatory guides. The acceptance criterion for empirical assessments is a demonstration that both the inner and outer container are not damaged in such a way that their performance in protecting the fuel assemblies during the thermal event is not compromised and the fuel itself is not damaged throughout the NCT and HAC certification testing. Additionally, package deformations obtained from certification testing are considered in subsequent thermal, shielding, and criticality evaluations are validated.

### **2.1.2.1 Analytic Design Criteria (Allowable Stresses)**

The allowable stress values used for analytic assessments of RAJ-II package structural performance come from the regulatory criteria such as yield strength or 1/3 of yield or from the ASME Code for the particular application. Material yield strengths, taken from the ASME Code, used in the analytic acceptance criteria,  $S_y$ , and ultimate strengths,  $S_u$ , are presented in Table 2 - 2 of Section 2.2.

### **2.1.2.2 Containment Structures**

The fuel cladding provides the primary containment for the nuclear fuel.

### **2.1.2.3 Non-Containment Structures**

For evaluation of lifting devices, the allowable stresses are limited to one-third of the material yield strength, consistent with the requirements of 10 CFR 71.45(a). For evaluation of tie-down devices, the allowable stresses are limited to the material yield strength, consistent with the requirements of 10 CFR 71.45(b).

### **2.1.2.4 Miscellaneous Structural Failure Modes**

#### **2.1.2.4.1 Brittle Fracture**

By avoiding the use of ferritic steels in the RAJ-II packaging, brittle fracture concerns are precluded. Specifically, most primary structural components are fabricated of austenitic stainless steel. Since this material does not undergo a ductile-to-brittle transition in the temperature range of interest (above -40 °F), it is safe from brittle fracture.

The closure bolts used to secure the inner and outer container lids are stainless steel, socket head cap screws ensuring that brittle fracture is not of concern. Other critical fasteners used in the RAJ-II packaging assembly provide redundancy and are made from stainless steel, again eliminating brittle fracture concerns.

#### **2.1.2.4.2 Extreme Total Stress Intensity Range**

Since the response of the RAJ-II package to accident conditions is typically evaluated empirically rather than analytically, the extreme total stress intensity range has not been quantified. Two full-scale certification test units (see Appendix 2.12.1) successfully passed free-drop and puncture testing. The CTUs were also fabricated in accordance with the drawings in Appendix 1.4.1, thus incurring prototypic fabrication induced stresses. Exposure to these conditions has demonstrated leak tight containment of the fuel, geometric configuration stability for criticality safety, and protection for the fuel. Thus the intent of the extreme total stress intensity range requirement has been met.

#### **2.1.2.4.3 Buckling Assessment**

Due to the small diameter of the containment boundary (the fuel rod cladding) and the fact that its radial deflection is limited by the internal fuel pellets, radial buckling is not a failure mode of concern for the containment boundary. Axial buckling deflection is also limited by the inner wall of the inner container and lid. The applied axial load to the fuel is also limited by the wood at the end of the packaging. The limited horizontal movement of the fuel during an end drop limits the ability of the fuel to buckle as demonstrated in tests performed on CTU 2 (see Appendix 2.12.1).

It is also noted that 30-foot drop tests performed on full-scale models with the package in various orientations produced no evidence of buckling of any of the fuel (see Appendix 2.12.1). Certification testing does not provide a specific determination of the design margin against buckling, but is considered as evidence that buckling will not occur. In addition buckling is a

potential concern to insure adequate geometric configuration control of the post accident package for criticality control. This involves not only the internal configuration of the package but the potential spacing between packages as well. Deformation of the RAJ-II is limited by its redundant structure. The wall of the package acts to stiffen the support plates that carry the load of the inner container via the vibration isolating mechanism. Part of the redundant system to minimize deformation of the fuel is the paper honeycomb that absorbs shocks that would impart side loading to the fuel. The inner container, consisting of an inner wall separated from an outer wall by thermal insulation, is lined with cushioning material that supports the fuel. Regardless of the specific failure mechanism of the support plates, the total deformation is limited by the shock absorbers (paper honeycomb). These blocks immediately share the load. Hence, even if the support plates would buckle allowing the outer wall to plastically deform, the amount of deformation is limited by the shock absorbing material. This has been demonstrated by test to allow only 118 mm (4.7 inches) of deformation of the shock absorbing blocks. The criticality evaluation takes into consideration this deformation. The redundant support system combined with the vibro-isolation and shock absorption system prevents the deformation of the inner container and the fuel.

The axial deformation resulting from an end drop is controlled in a similar manner. The end of the outer container has a wood shock absorber built in that carries the load from the inner container to the outer wall after the vibro-isolation device deflects. This reduces the load carried by the outer wall and support plates. It prevents large loads and deformations that could contribute to buckling of the fuel. The inner container constrains the fuel from large deformations or buckling.

Therefore, the support system prevents buckling of the packaging or fuel that would affect the criticality control or containment.

### **2.1.3 Weights and Centers of Gravity**

The maximum gross weight of a RAJ-II package, including a maximum payload weight of 684 kg (1,508 pounds) is 1,614 kg (3,558 pounds). The maximum vertical Center of Gravity (CG) is located 421 mm (16.57 inches) above the bottom surface of the package for a fully loaded package. A maximum horizontal shift of the horizontal CG is 92 mm (3.62 inches). This is allowed for in the lifting and tie-down calculations presented in Section 2.5.1. Figure 2-1 shows the locations of the center of gravity for the major components and the location of the center of gravity for the assembled. A detailed breakdown of the RAJ-II package component weights is summarized in Table 2 - 1.

#### **2.1.3.1 Effect of CG Offset**

The shift of the CG of the package 92 mm (3.6 inches) has very little effect on the performance of the package due to the length of the package, 5,068 mm (199.53 in). This results in a small shift of the weight and forces from one end of the package to the other. The actual total shift is:

$$3.6\% = 1 - \frac{(2)((5068 / 2) - 92)}{5068}$$

The offset of the CG is taken into account in the lifting and tie down calculations. The effect of this relatively small offset can be neglected.

## 2.1.4 Identification of Codes and Standards for Package Design

The radioactive isotopic content of the fuel is primarily U-235 with small amounts of other isotopes that make it Type B. Using the isotopic content limits shown in Section 1.2.3 the package would be considered a Category II. As such the applicable codes that would apply are the ASME Boiler and Pressure Vessel Code Section III, Subsection ND for the containment boundary which is the fuel cladding and Section III, Subsection NG for the criticality control Structure and the Section VIII for the non containment components.

The fuel cladding, due to its service in the reactor and need for high integrity, is designed to and fabricated to standards that exceed those required by ASME Section III Subsection ND. The structure used to maintain criticality control is demonstrated by test. The packaging capabilities are verified by test and the codes used in fabrication are called out on the drawings in Appendix 1.4.1. The sheet metal construction of the packaging requires different joint designs and manufacturing techniques that would normally be covered by the above referenced codes.

### 2.1.4.1 JIS/ASTM Comparison of Materials

The Certification Test Units (CTUs) were manufactured in Japan using material meeting JIS specifications. The fuel cladding and ceramic pellets were manufactured in the US to US specifications. The future manufacturing of RAJ-II packages may be performed using American standards (ASTM or ASME) that are appropriate substitutes for the Japanese standards (JIS) material comprising the CTUs. In order to assure that the packaging manufactured in the future meets the performance requirements demonstrated for the RAJ-II CTUs a detailed review of the differences between the American and Japanese standards was performed. The scope of the study included the: stainless steel products, wood products, rubber, paper honeycomb, and polyethylene foam. The study concluded that American standards material is available and compatible to the JIS standards. Future manufacturing of these packages for domestic use may be to American or Japanese specifications meeting the tolerances specified in the general arrangement drawings.

### 2.1.4.2 JIS/ASME Weld Comparison

Based upon an evaluation, it is concluded that the following standards are equivalent for the purposes of fabrication of the RAJ-II container in the United States:

Japanese Specification	American Specification
JIS Z 3821 Standard qualification procedure for welding technique of stainless steel	ASME Section IX
JIS Z 3140 Method of inspection for spot weld	ASME Section IX
JIS Z 3145 Method of bend test for stud weld	ASME Section IX

### 2.1.4.3 JIS/JSNDI/ASNT Non-destructive Examination Personnel Qualification and Certification Comparison

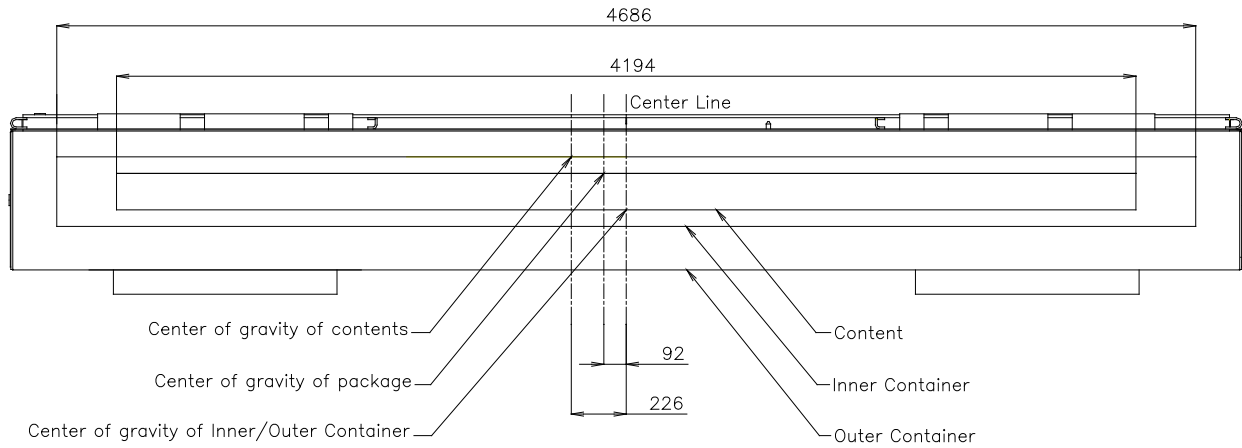
The following standards are considered equivalent for Non-destructive Examination Personnel Qualification and Certification. Personnel with these qualifications and certifications are authorized to perform examinations of the fabrication inspection requirements for the RAJ-II container in the United States. Although these documents cover other disciplines, this comparison only applies to Liquid Penetrant Examination.

<b>Japanese Specification</b>	<b>American Specification</b>
JIS Z 2305 Qualification and Certification for NDT Personnel	SNT-TC-1A* Recommended Practice
Certification NDIS 0601	SNT-TC-1A Recommended Practice
Certification NDIS J001	SNT-TC-1A Recommended Practice

\*Society of Non-destructive Testing – Technical Council

**Table 2 - 1 RAJ-II Weight**

Contents	Number of assemblies per package	Maximum 2 Assemblies
	Number of fuel rods per package	Maximum 130 (See Table 6.2)
	Total weight	684 kg (1,508 lb)
Inner container	Body	200 kg (441 lb) (including bolts)
	Lid	101 kg (223 lb)
	End lids	7 kg (15.4 lb)
	Total weight	308 kg (679 lb)
Outer container	Body	485 kg (1,069 lb) (including bolts)
	Lid	137 kg (302 lb)
	Total weight	622 kg (1,371 lb)
Total weight of package		1,614 kg (3,558 lb)



(unit: mm)

**Figure 2-1 Center of Gravity of Package Components**

## 2.2 MATERIALS

### 2.2.1 Material Properties and Specifications

The major structural components, i.e., the Outer Container (OC) and Inner Container (IC) walls, supports, and attachment blocks are fabricated from austenitic stainless steel. Other materials performing a structural function are lumber (bolster), balsa (shock absorber), paper honeycomb (shock absorber), alumina silicate (thermal insulator), polyethylene foam (cushioning material), and zirconium alloy (fuel rod cladding). The drawings presented in Appendix 1.4.1 delineate the specific material(s) used for each RAJ-II packaging.

The remainder of this section presents and discusses pertinent mechanical properties for the materials that perform a structural function. Both the materials that are used in the analytics and those whose function in the package is demonstrated by test such as the shock absorbing material are presented. In general the analytics covering the lifting and tie down capabilities of the package and some normal condition events are limited to the stainless steel structure of the packaging.

Table 2 - 2 presents the bounding mechanical properties for the series 300 stainless steel used in the RAJ-II packaging. Each of the representative mechanical properties is those of Type 304 stainless steel and is taken from Section II, Parts A and D, of the ASME Boiler and Pressure Vessel Code. These properties are applicable to both packages that may have been made in Japan to Japanese specifications, Japanese Industrial Standards (JIS) or using ASME specification material. The density of stainless steel is taken as 0.29 lb/in<sup>3</sup> (8.03E3 kg/m<sup>3</sup>), and Poisson's Ratio is 0.3.

Table 2 - 3 presents the mechanical properties of the main non-stainless steel components of the package necessary for the structural analysis.

**Table 2 - 2 Representative Mechanical Properties of 300 Series  
Stainless Steel Components**

① Minimum Elongation (%)	Temperature °C (°F)	② Yield Strength, $S_y$ MPa ( $\times 10^3$ psi)	③ Ultimate Strength, $S_u$ MPa ( $\times 10^3$ psi)	④ Elastic Modulus, E GPa ( $\times 10^6$ psi)	⑤ Thermal Expansion Coefficient, $\alpha$ $\times 10^{-6}$ mm/mm/°C ( $\times 10^{-6}$ in/in/°F)
35	-29 (-20)	206.8 (30.0)	517.1 (75.0)	-----	-----
40	21 (70)	206.8 (30.0)	517.1 (75.0)	195.1 (28.3)	-----
30	38 (100)	206.8 (30.0)	517.1 (75.0)	-----	15.39 (8.55)
25	93 (200)	172.4 (25.0)	489.5 (71.0)	190.3 (27.6)	15.82 (8.79)
30	149 (300)	155.1 (22.5)	455.1 (66.0)	186.2 (27.0)	16.2 (9.00)
40	204 (400)	142.7 (20.7)	444.0 (64.4)	182.7 (26.5)	16.54 (9.19)
40 <sup>⑥</sup>	23°C <sup>⑥</sup>	205 MPa Min <sup>⑥</sup>	520 MPa Min <sup>⑥</sup>	-----	-----
40 <sup>⑦</sup>	21°C <sup>⑦</sup>	205 MPa Min <sup>⑦</sup>	515 MPa Min <sup>⑦</sup>	-----	-----

- Notes:
- ① ASME Code, Section II, Part A
  - ② ASME Code, Section II, Part D, Table Y-1.
  - ③ ASME Code, Section II, Part D, Table U
  - ④ ASME Code, Section II, Part D, Table TM-1, Material Group G.
  - ⑤ ASME Code, Section II, Part D, Table TE-1, 18Cr-8Ni, Coefficient B.
  - ⑥ JIS Handbook Ferrous Materials and Metallurgy I, Sections G4303, G4304, G4305 Material Specifications
  - ⑦ ASTM A240, A666 & A276 Material Specifications

**Table 2 - 3 Mechanical Properties of Typical Components**

Materials (Usage)	Yield stress or yield strength	Tensile strength	Compressive strength	Bending strength	Static initial peak stress	Modulus of longitudinal elasticity	Density (g/cm <sup>3</sup> )
Lumber (bolster)	56.3 MPa Nominal	–	50.5 MPa Nominal	72.0 MPa Nominal	–	7.85 GPa Nominal	0.53 Nominal
Balsa (shock absorber)	–	–	16 MPa Nominal	–	–	–	0.18 Nominal
Paper honeycomb (shock absorber)	–	–	–	–	2.35 MPa Nominal	–	0.06 Nominal
Alumina Silicate (thermal insulator)	–	–	294 kPa Nominal	314 kPa Nominal	–	–	0.25 Nominal
Foam polyethylene (cushioning mat'l)	–	–	Approx. 0.2MPa @ 50% strain	–	0.69 MPa Nominal	–	0.068 Nominal
Zirconium alloy (fuel rods) ASTM B811	241 MPa (35,000psi)	413 MPa (60,000psi)	–	–	–	97.1 GPa Nominal	6.5 Nominal
300 Series Stainless Socket Headed Cap screw	241 MPa (35,000psi) (Min)	379 MPa (75,000psi) (Min)	–	–	–	–	–

### 2.2.2 Chemical, Galvanic, or Other Reactions

The major materials of construction of the RAJ-II packaging (i.e., austenitic stainless steel, polyurethane foam, alumina thermal insulator, resin impregnated paper honeycomb, lumber

(hemlock and balsa), and natural rubber) will not have significant chemical, galvanic or other reactions in air, inert gas or water environments, thereby satisfying the requirements of 10 CFR 71.43(d). These materials have been previously used, without incident, in radioactive material (RAM) packages for transport of similar payload materials. A successful RAM packaging history combined with successful use of these fabrication materials in similar industrial environments ensures that the integrity of the RAJ-II package will not be compromised by any chemical, galvanic, or other reactions.

The RAJ-II packaging is primarily constructed of series 300 stainless steel. This material is highly corrosion resistant to most environments. The metallic structure of the RAJ-II packaging is composed entirely of this material and compatible 300 series weld material. Since both the base and weld materials are 300 series materials, they have nearly identical electrochemical potential thereby minimizing any galvanic corrosion that could occur.

The stainless steel within the IC cavity between the inner and outer walls is filled with a ceramic alumina silicate thermal insulator. This material is non-reactive with either the wood or the stainless steel, both dry or in water. The alumina silicate is very low in free chlorides to minimize the potential for stress corrosion of the IC structure.

The polyethylene foam that is used in the IC for cushioning material has been used previously and is compatible with stainless steel. The polyethylene foam is very low in free halogens and chlorides.

Resin impregnated paper honeycomb is used in the RAJ-II packaging as cushioning material. The impregnated paper is resistant to water and break down. It is low in leachable halides.

The natural rubber that is used as a gasket for the lids and in the vibro-isolating system, contains no corrosives that would react adversely affect the RAJ-II packaging. This material is organic in nature and non-corrosive to the stainless steel boundaries of the RAJ-II packaging.

### **2.2.2.1 Content Interaction with Packaging Materials of Construction**

The materials of construction of the RAJ-II packaging are checked for compatibility with the materials that make up the contents or fuel rods that are to be shipped in the RAJ-II. The primary materials of construction of the fuel assembly that could come in contact with the packaging are the stainless steel and the zirconium alloy material that is used for the cladding of the fuel rods. Zirconium alloy (including metal zirconium), stainless steel, and Ni-Cr-Fe alloy, which form a passivated oxide film on the surface under normal atmosphere with slight moisture, are essentially stable. The contact of the above three kinds of metals with polyethylene is chemically stable. These materials are compatible with the stainless steel, polyethylene, and natural rubber that could come in contact with the contents.

### **2.2.3 Effects of Radiation on Materials**

Since this is an unirradiated fuel package, the radiation to the packaging material is insignificant. Also, the primary materials of construction and containment, austenitic stainless steel and the zirconium alloy cladding of the fuel are highly resistant to radiation.

## **2.3 FABRICATION AND EXAMINATION**

### **2.3.1 Fabrication**

The RAJ-II is fabricated using standard fabrication techniques. This includes cutting, bending and welding the stainless steel sheet metal. As shown on the drawing the welding is done to AWS D1.6 Welding of Stainless Steel. The process may also be controlled by ASME Section IX or other international codes. The containment, the cladding of the fuel rods is fabricated to standards that exceed the required Section VIII of the ASME Boiler and Pressure vessel code do to the service requirements of the fuel in reactors.

### **2.3.2 Examination**

The primary means of examination to determine compliance of the RAJ-II to the design requirements is visual examination of each component and the assembled units. This includes dimensional verification as well as material and weld examination. The materials will also be certified to the material specifications. Shock absorbing material such as the paper honeycomb will also have verified material properties.

## **2.4 LIFTING AND TIE-DOWN STANDARDS FOR ALL PACKAGES**

For analysis of the lifting and tie-down components of the RAJ-II packaging, material properties from Section 2.2 are taken at a bounding temperature of 75°C (167 °F) per Section 2.6.1.1. This is the maximum temperature that the container reaches when in the sun. The primary structural material is 300 series stainless steel that is used in the Outer Container (OC).

A loaded RAJ-II package can be lifted using either a forklift or by slings. The gross weight of the package is a maximum of 1,614 kg (3,558 lbs). Locating/protection plates for the forklift and locating angles for the sling locate the lift points for the package. In both cases the package is lifted from beneath. The failure of these locating/protective features would not cause the package to drop nor compromise its ability to perform its required functions.

The inner container may be lifted empty or filled with the contents using the sling fittings that are attached at the positions shown in Figure 2-2. The details of the sling fittings are as shown in Figure 2-3. Since the center of gravity depends on existence of the contents, the sling fittings for the filled container and the empty container are marked respectively as "Use When Loaded" and

"Use When Empty" to avoid improper operations. Also, the sling fittings on the lid of inner container to lift the lid only are marked as "Use for Lifting Lid" similar to the outer container.

The sling devices are mechanically designed to be able to handle the package and the inner container filled with the fuel assemblies in safety; they can lift three times the gross weight of the package, or three times the gross weight of the filled inner container respectively, so that they can with stand rapid lifting.

Properties of 300 series stainless steel are summarized below.

**Table 2 - 4 Properties of 300 Series Stainless Steel**

Material Property	Value	Reference
<b>At 75°C (167 °F)</b>		
Elastic Modulus, E	191.7 GPa ( $27.8 \times 10^6$ psi)	Table 2 - 2
Yield Strength, $\sigma_y$	184.7 MPa (26,788 psi)	
Shear Stress, equal to (0.6) $\sigma_y$	110.8 MPa (16,073 psi)	

### 2.4.1 Lifting Devices

This section demonstrates that the attachments designed to lift the RAJ-II package are designed with a minimum safety factor of three against yielding, per the requirements of 10 CFR71.45 (a).

The lifting devices on the outer container lid are restricted to only lifting the outer container lid, and the lifting devices in the inner lid are restricted to only lifting the inner container lid. Although these lifting devices are designed with a minimum safety factor of three against yielding, detailed analyses are not specifically included herein since these lifting devices are not intended for lifting a RAJ-II package.

The outer container can be handled by either forklift or slings in a basket hitch around the package, requiring no structural component whose failure could affect the performance of the package.

### 2.4.1.1 Lifting of Inner Container

The inner container is lifted when loaded with fuel from the outer container with sling fittings attached to the body of the inner container. Three pairs (six in total) of the sling fittings are attached to the inner container as shown in Figure 2-2. The center of gravity depends upon whether the container is filled or not. Since the six sling fittings are the same, the stress in the sling fittings are evaluated for the case of at the maximum weight condition that occurs when the inner container is filled with fuel assemblies.

The stress on the sling fitting when lifting the inner container filled with contents is evaluated by determining the maximum load acting on any given fitting.

The maximum load,  $P_v$ , (see Figure 2-9) acting on one of the sling fitting vertically when lifting is given by the following equation:

$$P_v = \frac{(W_2 + W_3)}{n} \cdot g$$

where

$P_v$ : maximum load acting to sling fitting in vertical direction	N
$W_2$ : mass of inner container	308 kg (679 lb)
$W_3$ : mass of contents	684 kg (1,508 lbs)
$n$ : number of sling fittings	4
$g$ : acceleration of gravity	9.81 m/s <sup>2</sup>

Accordingly, the maximum load acting on the sling fitting vertically is calculated as

$$P_v = \frac{684 + 308}{4} \times 9.81 = 2.433 \times 10^3 \text{ N (546.9 lbf)}$$

The load,  $P$ , acting to the sling fitting when the sling is at a minimum angle of 60° is calculated as

$$P = \frac{P_v}{\sin \theta} = \frac{2.433 \times 10^3}{\sin 60^\circ} = 2.809 \times 10^3 \text{ N (631 lbf)}$$

Also, the maximum load,  $P_H$ , acting on the sling fitting horizontally is calculated as:

$$P_H = \frac{P_v}{\tan \theta} = \frac{2.433 \times 10^3}{\tan 60^\circ} = 1.405 \times 10^3 \text{ N (316 lbf)}$$

Each sling fitting is made up of a hooking bar which is a 12mm diameter bent rod and a perforated plate that is made up of two pieces of angle that are welded together. The perforated plate of the sling fitting is welded to a support of that is welded to the body of the inner container.

The shearing stress in the hooking bar (see Figure 2-6) is given by the following equation:

$$\tau_N = \frac{P \times \phi}{A}$$

Where

$\tau_N$ : shearing stress on hooking bar of sling fitting MPa

P: maximum load  $2.809 \times 10^3 \text{ N (631 lbf)}$

A: cross-section of hooking bar of sling fitting  $\pi/4 \times 12^2 = 113 \text{ mm}^2 (0.175 \text{ in}^2)$

$\phi$ : load factor 3

Accordingly, the shearing stress on the hooking bar of the sling fitting at its center is calculated as

$$\tau_N = \frac{2.809 \times 10^3 \times 3}{113} = 74.58 \text{ MPa (10,820 psi)}$$

The yield stress for stainless steel is 184.7 MPa (26,790 psi) and the shear allowable is  $0.6 \times 184.7 = 110.8 \text{ MPa (16,070 psi)}$  at the maximum normal temperature, hence the margin (MS) is

$$\text{MS} = \frac{110.8}{74.58} - 1 = 0.48$$

Therefore, the sling fitting can withstand three times the load without yielding in shear.



$$I_X = I_{X2} - I_{X1}$$

$$I_Y = \Sigma I_{Yi}$$

where

$I_p$  : moment of inertia of area to welds  $\text{mm}^4$

$I_X$  : moment of inertia of area to welds for X-axis  $\text{mm}^4$

$I_Y$  : moment of inertia of area to welds for Y-axis  $\text{mm}^4$

$I_{X1}$  : moment of inertia of area to inside of weld for X-axis  $\text{mm}^4$

$I_{X2}$  : moment of inertia of area to outside of weld for X-axis  $\text{mm}^4$

$I_{Y1}$  : moment of inertia of area to each weld for Y-axis  $\text{mm}^4$

The moment of inertia of area,  $I$ , to a cross-sectional area of width,  $b$ , and height,  $h$ , is given by:

$$I = \frac{1}{12} bh^3$$

Conservatively only the outside welds not including any corner wrap around that attach the sling fitting to the support plate are considered. Thus, the moment of inertia of area,  $I_X$  and  $I_Y$  to the welds for X-axis and Y-axis are calculated as:

$$I_X = \left(\frac{1}{12} \times 88 \times 54^3\right) - \left(\frac{1}{12} \times 88 \times 50^3\right) = 2.38 \times 10^5 \text{ mm}^4 (0.57 \text{ in}^4)$$

$$I_Y = 2I_{Y1} = 2 \times \frac{1}{12} \times 2 \times 88^3 = 2.27 \times 10^5 \text{ mm}^4 (0.55 \text{ in}^4)$$

Accordingly, the moment of inertia of area,  $I_p$ , to the welds is calculated as

$$I_p = (2.38 \times 10^5) + (2.27 \times 10^5) = 4.65 \times 10^5 \text{ mm}^4 (1.12 \text{ in}^4).$$

The shearing stress,  $S_d$ , on the weld due to the load acting on the sling fitting is given by the following equation:

$$S_d = \frac{P \cdot \phi}{A}$$

Where:

$S_d$ : shearing stress on welds due to the load to sling fitting                      MPa

P: maximum load acting to one of sling fitting                       $2.809 \times 10^3$  N (631 lbf)

A: overall cross-section of welds                       $2 \times 88 = 176$  mm<sup>2</sup> (0.273 in<sup>2</sup>)

$\phi$ : load factor                      3

Accordingly, the shearing stress on welds due to the load acting to the sling fitting is calculated as:

$$S_d = \frac{2.809 \times 10^3 \times 3}{176} = 47.9 \text{ MPa (6,950 psi)}$$

The maximum bending moment acting to the sling fitting is given by the following equation from Figure 2-9

$$M_{\max} = P \cdot l$$

Where:

$M_{\max}$ : maximum bending moment acting to sling fitting                      N · mm

P: maximum load acting to one of sling fitting                       $2.809 \times 10^3$  N (631 lbf)

l: distance from fulcrum to load point                      17 mm (0.67 in)

Therefore, the maximum bending moment acting to the sling fitting is calculated as:

$$\begin{aligned} M_{\max} &= 2.809 \times 10^3 \times 17 \\ &= 4.8 \times 10^4 \text{ N}\cdot\text{mm (424.8 in}\cdot\text{lbf)} \end{aligned}$$

The stress due to this bending moment is given by the following equation:

$$S_m = \frac{M_{\max} \cdot r \cdot \phi}{I_p}$$

Where:

$S_m$ : Stress acting to a point at r from center of gravity due to bending moment

MPa

r: distance from center of gravity to end of welds  $\sqrt{44^2 + 25^2} = 50.6$  mm (1.99 in)

$M_{\max}$ : maximum bending moment acting to sling fitting

$4.8 \times 10^4$  N·mm (424.8 in·lbf)

$I_p$ : moment of inertia of area to welds

$4.65 \times 10^5$  mm<sup>4</sup> (1.12 in<sup>4</sup>)

$\phi$ : load factor

3

From this equation, the maximum bending moment,  $S_m$ , acting to the sling fitting is calculated as:

$$S_m = \frac{4.8 \times 10^4 \times 50.6 \times 3}{4.65 \times 10^5} = 15.6 \text{ MPa (2,260 psi)}$$

In addition, the composite shearing stress, S, on the welds is given by the following equation:

$$S = \sqrt{S_d^2 + S_m^2 + 2S_d S_m \cos\theta}$$

Where:

$$\cos\theta = 25/50.6$$

From this equation, the composite shearing stress, S, is calculated as

$$S = \sqrt{47.9^2 + 15.6^2 + 2 \times 47.9 \times 15.6 \times 25 / 50.6}$$

$$= 57.2 \text{ MPa (8,300 psi)}$$

Meanwhile, the allowable shearing stress for 300 series stainless steel is 110.8 MPa (16,073 psi).

Then the margin (MS) is:

$$MS = \frac{110.8}{57.2} - 1 = 0.94$$

The welds are capable of carrying 3 times the expected load without yielding.

Likewise the welds of the support plates for sling fittings are evaluated in the same manner. Since the welds of the support plates (see Figure 2-10) receive the same load as mentioned above in the case of the welds of the sling fittings, it is evaluated by same analytic method as mentioned above. The symbols used here shall have same meaning.

The moment of inertia of area,  $I_p$ , to the welds of support plate is given by the following equation:

$$I_p = I_x + I_y$$

Where:

$$I_x = I_{x2} - I_{x1}$$

$$I_y = I_{y2} - I_{y1}$$

The moment of inertia of areas  $I_x$  and  $I_y$  to the welds for X-axis and Y-axis are calculated as:

$$\begin{aligned} I_x &= \frac{1}{12} \times 153 \times 83^3 - \frac{1}{12} \times 150 \times 80^3 \\ &= 8.903 \times 10^5 \text{ mm}^4 (2.14 \text{ in}^4) \end{aligned}$$

$$\begin{aligned} I_y &= \frac{1}{12} \times 83 \times 153^3 - \frac{1}{12} \times 80 \times 150^3 \\ &= 2.273 \times 10^6 \text{ mm}^4 (5.46 \text{ in}^4) \end{aligned}$$

Accordingly, the moments of inertia of areas to the welds for the support plates are calculated as:

$$\begin{aligned} I_p &= 8.903 \times 10^5 + 2.273 \times 10^6 \\ &= 3.163 \times 10^6 \text{ mm}^4 (7.60 \text{ in}^4) \end{aligned}$$

The overall cross-section, A, of welds of the support plate is:

$$\begin{aligned} A &= (153 \times 83) - (150 \times 80) \\ &= 699 \text{ mm}^2 (1.08 \text{ in}^2) \end{aligned}$$

The shearing stress,  $S_d$ , on the welds of the support plate for the sling fitting is calculated by a similar equation as the welds of the sling fitting.

$$S_d = \frac{2.809 \times 10^3 \times 3}{699} = 12.1 \text{ MPa (1,760 psi)}$$

In addition, the stress,  $S_m$ , on the welds of the support plate due to the bending moment is calculated as:

Where:

$$r = \sqrt{75^2 + 40^2} = 85 \text{ mm (3.35 in)}$$

$$S_m = \frac{5.9 \times 10^4 \times 85 \times 3}{3.163 \times 10^6} = 4.76 \text{ MPa (690 psi)}$$

Accordingly, the composite shearing stress  $S$  on the welds of support plate is calculated as:

$$S = \sqrt{S_d^2 + S_m^2 + 2S_d S_m \cos\theta}$$

Where:

$$\cos \theta = 40/85$$

$$\begin{aligned} S &= \sqrt{12.1^2 + 4.76^2 + (2 \times 12.1 \times 4.76 \times (40/85))} \\ &= 14.9 \text{ MPa (2,160 psi)} \end{aligned}$$

Meanwhile, the allowable shearing stress for 300 series stainless steel is 110.8 MPa (16,073 psi). Then the margin of safety (MS) is:

$$MS = \frac{110.8}{14.9} - 1 = 6.4$$

Therefore, the support plate welds are capable of carrying three times the normal load and no yielding.

As indicated by the margins of safety calculated for each component, the hook bar has the lowest margin; therefore in case of an overload the hook bar will fail prior to any other component. This ensures that, at failure, the rest of the packaging is capable of performing its function of protecting the fuel.

#### 2.4.1.2 Package Lifting Using the Outer Container Lid Lifting Lugs

The outer container lid is lifted by four (4) Ø8-mm (Ø0.315 in.) Type 304 stainless steel bars that are welded to the 50 × 50 × 4 stainless steel lid flange angle. Under a potential excessive loading condition, such as lifting the entire loaded package, these four lifting lugs are required to fail prior to damaging the outer container lid structure.

The outer container lid is also equipped with the four (4) Ø6-mm (Ø0.236 in.) Type 304 stainless steel bar handles, which may be used to manually lift the lid. These bars are welded to the vertical leg of the lid flange angle with single-sided flare-bevel welds for an approximate length of 13 mm, as shown in View G-G on General Arrangement Drawing 105E3743. Since the handles have smaller cross-section (Ø6-mm vs. Ø8-mm), and have smaller and shorter attachment welds, the analysis of the lid lifting bars bounds the handles.

The four lifting bars will be used for this analysis with an assumed lifting angle of 45 degrees. From Table 2-1, the RAJ-II package weighs 1,614 kg [15,827 N] (3,558 lbs). For the assumed lifting arrangement, the maximum load on the bar is:

$$F = 1/4 \left[ \frac{15,827}{\sin 45^\circ} \right] = 5,596 \text{ N (1,258 lbs)}$$

Assuming that the lift point is centered above the midpoint of the package (located 1,025 mm longitudinally and 318 mm laterally from lifting bar), the resultant forces on the lifting bar will be:

$$F_{\text{horizontal}} = F_{\text{vertical}} = F \cos 45^\circ = 3,957 \text{ N (890 lbs)}$$

$$F_{//} = F_{\text{horizontal}} \sin\left(\tan^{-1}\left(\frac{1,025}{318}\right)\right) = 3,779 \text{ N (850 lbs)}$$

$$F_{\perp} = F_{\text{horizontal}} \cos\left(\tan^{-1}\left(\frac{1,025}{318}\right)\right) = 1,173 \text{ N (264 lbs)}$$

where:  $F_{\text{horizontal}}$  = Force in horizontal plane  
 $F_{//}$  = Force parallel to longitudinal axis of package  
 $F_{\perp}$  = Force perpendicular to longitudinal axis of package

These reaction loads will develop both bending and shear stresses in the bar, shear stresses in the attachment welds, and tensile stresses in the flange angle. Each of these stress components will be analyzed separately.

#### **Bending of Bar**

The maximum reaction load on the lifting bar will be bending stresses in the bar. Treating the bar as a fixed-fixed beam, the maximum bending stress,  $\sigma_b$ , will be:

$$\sigma_b = \frac{M_{\max}}{Z_{\text{bar}}}$$

where:  $M_{\max} = 1/8[(F_{\text{vertical}})^2 + (F_{//})^2]^{1/2}(l) = 1/8(5,472)(76) = 51,984 \text{ N-mm (460 lb}_f\text{-in)}$   
 $Z_{\text{bar}} = \pi(d^3)/32 = \pi(8^3)/32 = 50.3 \text{ mm}^3 \text{ (0.003 in}^3\text{)}$   
 $l = 2(46-8) = 76 \text{ mm (2.99 in)}$  [assumed equal to bent free length of bar]

Substituting these values results in a maximum bending stress of 1,033 MPa (149,824 psi). The allowable bending stress for the Type 304 material is equal to  $S_y = 184.7 \text{ MPa (26,788 psi)}$ . Therefore, the margin of safety against yielding in bending is:

$$\text{MS} = \frac{184.7}{1,033} - 1.0 = -0.8$$

### **Shear of Bar**

The maximum reaction load on the lifting bar will result in shear stresses in the bar. For the shearing the bar, the maximum shear stress will be:

$$\tau_{\text{bar}} = \frac{[(F_{\text{vertical}})^2 + (F_{//})^2]^{1/2}}{\text{Area}} = \frac{5,472}{(\pi/4)(8)^2} = 108.9 \text{ MPa (15,795 psi)}$$

The allowable shear stress for the Type 304 material is equal to  $0.6S_y = 0.6(184.7) = 110.8 \text{ MPa (16,070 psi)}$ . Therefore, the margin of safety against yielding in shear is:

$$\text{MS} = \frac{110.8}{108.9} - 1.0 = +0.02$$

### **Tension in Bar**

Since the bending stress is well beyond the yield strength, the bar will bend until the reaction load will be reacted as pure tension in the bar. For this condition, the tensile stress,  $\sigma_{\text{t-bar}}$ , in the bar will be:

$$\sigma_{\text{t-bar}} = \frac{F}{2(\text{Area})} = \frac{5,596}{2[(\pi/4)(8^2)]} = 55.7 \text{ MPa (8,079 psi)}$$

The allowable tensile stress for the Type 304 material is equal to the minimum yield strength, 184.7 MPa (26,788 psi). The margin of safety for this condition is then:

$$\text{MS} = \frac{184.7}{55.7} - 1.0 = +2.3$$

### **Attachment Welds**

As shown in View F-F on General Arrangement Drawing 105E3743, the lifting bars are welded to the lid flange angle with double-sided flare-bevel welds for an approximate length of 28 mm (1.10 in.) on each leg of the bar. The ends of the bar are welded with a seal fillet weld, which has minimal strength and hence, will be ignored. Since the bar is relatively small, the flare-bevel weld will be treated as an equivalent fillet weld with a 4-mm leg. For this assumption, the maximum primary shear stress,  $\tau_{\text{weld}}$ , in the weld will be:

$$\tau_{\text{weld}} = \frac{[(F_{\text{vertical}})^2 + (F_{//})^2]^{1/2}}{\text{Shear area of welds}} = \frac{5,472}{4(4 \cos 45^\circ)(28)} = 17.3 \text{ MPa (2,509 psi)}$$

Due to the off-set, there will also be a secondary (torsion) shear stress,  $\tau'_{\text{weld}}$ , component:

$$\tau'_{\text{weld}} = \frac{Mr}{J}$$

where:  $M$  = applied moment to weld group  
 $= [(F_{\text{vertical}})^2 + (F_{//})^2]^{1/2}$  (distance from centroid + bend radius +  $\frac{1}{2}$ bar diameter)  
 $= 5,472(14 + 8 + 4) = 142,272 \text{ N}\cdot\text{mm}$  (1,259  $\text{lb}_f \cdot \text{in}$ )  
 $r_{\text{max}}$  = distance from centroid of weld group to farthest point in weld  
 $= [(1/2(46-8))^2 + (14)^2]^{1/2} = 23.6 \text{ mm}$  (0.929 in)  
 $J$  = second polar moment of inertia of weld group,  $\text{mm}^4$

Since the four flare-bevel welds are the same size and location, the second polar moment of inertia for the weld group is determined treating the welds as a line<sup>a</sup>. For this case, the second polar moment of inertia is:

$$J = 0.707(h) \frac{d(3b^2 + d^2)}{6}$$

where:  $h$  = leg length of weld = 4 mm  
 $d$  = length of weld = 28 mm  
 $b$  = distance between weld groups =  $(46^2 + 46^2)^{1/2} = 65.1 \text{ mm}$

Substituting these values results in a secondary polar moment of inertia of  $178,138 \text{ mm}^4$  (0.428  $\text{in}^4$ ). The secondary shear stress then becomes:

$$\tau'_{\text{weld}} = \frac{(142,272)(23.6)}{178,138} = 18.8 \text{ MPa} (2,727 \text{ psi})$$

The total shear stress in the weld is then the square root of the sum of the squares of the primary shear and secondary shear:

$$\tau_{\text{total}} = \left[ (\tau_{\text{weld}})^2 + (\tau'_{\text{weld}})^2 \right]^{1/2} = 25.5 \text{ MPa} (3,698 \text{ psi})$$

The allowable shear stress for the Type 304 material is equal to 110.8 MPa (16,070 psi). Therefore, the margin of safety against yielding in shear for the welds is:

$$\text{MS} = \frac{110.8}{25.5} - 1.0 = +3.3$$

### **Shear Tearout of Base Metal**

Shear tearout of the 4-mm thick base metal is evaluated by conservatively considering only the area of a section equal to the weld length of the two welds. The 2-mm thick sheet that is attached to the vertical leg of the flange angle is ignored for this calculation. The total tensile area,  $A_t$ , will be:

$$A_{\text{shear}} = 2[4(28)] = 224 \text{ mm}^2 (0.347 \text{ in}^2)$$

For this case, the shear stress of the base metal,  $\tau_{\text{base metal}}$ , is:

<sup>a</sup>Shigley, Joseph E., and Mischke, Charles R., *Mechanical Engineering Design, Fifth Edition*, McGraw-Hill, Inc., 1989.

$$\tau_{\text{base metal}} = \frac{F}{A_{\text{shear}}} = \frac{5,596}{224} = 25.0 \text{ MPa (3,624 psi)}$$

The allowable shear stress for the Type 304 material is equal to 110.8 MPa (16,070 psi). The margin of safety for this condition is then:

$$\text{MS} = \frac{110.8}{25.0} - 1.0 = +3.4$$

### **Summary**

As demonstrated by these calculations, the minimum margin of safety for the outer container lid lifting lugs is -0.8, which results in failure of the bar in bending for lifting the complete loaded package. The largest positive margin of safety (+3.4) occurs in the base metal of the lid flange angle, which demonstrates that the outer container lid structure would not fail in an excessive load condition. All other margins of safety in the load path are positive, but are lower than the base metal. Therefore, potentially lifting the complete package by these lid lifting lugs will fail the lifting bar and have no detrimental affect on the effectiveness of the RAJ-II package.

### **2.4.2 Tie-Down Devices**

There are no tie-down features that are a structural part of the RAJ-II package. The packages are transported either in container vans or on flatbed trucks. When transported in container vans, blocking and bracing is provided that distributes any loads into the packages. This bracing and blocking is customized to address individual shipping configurations and the specific container van being used. When transported on a flatbed trailer, straps going over the package are used to secure it to the trailer. Therefore, the requirements of 10 CFR 71.45(b) are satisfied since no structural part of the package is used as a tie-down device.

An evaluation is performed on the ability of the package to withstand loadings of 2g vertical and 5 g laterally when restrained by strapping. The worst case loading situation for the packages is when they are stacked in groups of 9 on a flatbed trailer and secured with a minimum of 3 straps. Although the packages may be shipped in other configurations such as 2x3 the greatest strap loading that would be applied to the package when secured in a 3x3 configuration. Between each adjacent column of packages 2 x 4 wood shoring may be placed where the straps will be applied. The evaluation below is conservatively performed without the 2 x 4 shoring in place.

As a bounding evaluation, it is assumed that the outside corners of the top outside packages carry all the vertical loads that would result from the vertical acceleration and the vertical load required to resist the over-turning moment from the horizontal acceleration. The corners of all top packages would actually carry the vertical load. See Figure 2-11.

For modeling purposes, the matrix of nine packages is treated as a rigid body. By summing moments, the vertical force required to prevent the over-turning of the stack by the horizontal loads is determined. This load is conservatively applied to one edge of one container

The key dimensions and weights for each package are:

Width	w = 720 mm (28.3in)
Total Height	h = 742 mm (29.2in)

CG height	$cgy = 421 \text{ mm (16.6 in)}$
Mass of each package	$m = 1,614 \text{ kg (3,558 lb)}$
Gravitational acceleration	$g = 9.81 \text{ m/sec}^2$
Vertical acceleration factor	$g_v = 2$
Horizontal acceleration factor	$g_h = 5$

The vertical center of gravity of the 9-package matrix is:

$$CG_y = 3mg(2h + cgy)/9mg + 3mg(h + cgy)/9mg + 3mg(cgy)/9mg = 1.163 \times 10^3 \text{ mm (45.8 in)}$$

Summing the forces in the vertical direction due to the 2 g loading, the strap load applied at the two locations can be determined for this load condition.

$$R_{st} = 9 g_v m g/2 = 1.425 \times 10^5 \text{ N (3.202} \times 10^4 \text{ lb}_f)$$

Summing moments about one of the bottom corners of the stack will determine the strap force required to resist overturning due to the horizontal loading.

$$R_s = \frac{(g_h(CG_y)9mg)}{(3w)} = 3.835 \times 10^5 \text{ N (8.621} \times 10^4 \text{ lb}_f)$$

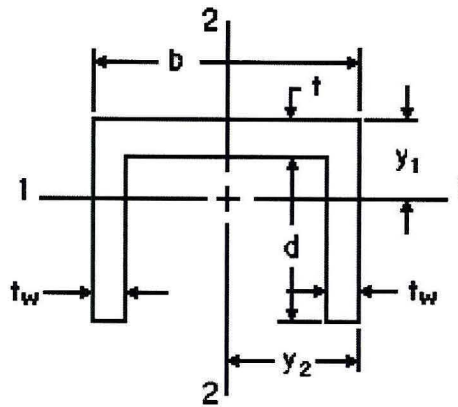
Total vertical strap load is:

$$R_t = R_{st} + R_s = 5.260 \times 10^5 \text{ N (1.182} \times 10^5 \text{ lb}_f)$$

Checking the support plate carrying capability:

There are eight (8) 5mm × 55mm support plates in groups of two (2) that carry the vibro-isolation frame inside the outer container. These are skipped welded to the wall, plus have two thick (10 and 15 mm) by 80 mm and 70 mm wide plates welded between them. These plates are in addition to the body straps and the body struts (angles) in corners that provide vertical stiffening to the side panels. On top of the side panel, there are two angles that make up the flange in both the body and the lid that provide load distribution capability to the side wall and the internal structure. In addition these angles are stiffen at the ends by the bolster support angle that further distributes the end strap loads to the end structure of the package reducing load in the sides of the package.

Since the eight support plates are assembled together in groups of two with the reinforcement plates connecting the plates along with the welding to the wall, each two-plate section is considered as a column that is capable of carrying the tie-down loads. Addressing the support plates as a channel section, which is 140 mm wide and 57 mm deep, its properties can be determined.



Channel section

Length of web  $b = 140 \text{ mm (5.5 in)}$

Length of flange  $d = 55 \text{ mm (2.2 in)}$

Web thickness  $t = 2 \text{ mm (0.08 in)}$

Flange thickness  $t_w = 5 \text{ mm (0.2 in)}$

Area  $A = t_b + 2t_w d = 830.3 \text{ mm}^2 (1.287 \text{ in}^2)$

Since there are four of these assemblies to a side the total area is:

$$A_{\text{spt}} = 4A = 3,321 \text{ mm}^2 (5.148 \text{ in}^2)$$

The compressive stress is:

$$\sigma_c = R_t / A_{\text{spt}} = 158.4 \text{ MPa (23.0 ksi)}$$

This is less than the yield stress of the Type 304 stainless steel  $S_y = 206.8 \text{ MPa (30.0 ksi)}$

The resistance of the plate to buckling is also evaluated. The equation to obtain the moments of inertia of area of the support plate which are subject to buckling is:

$$y_1 = (bt^2 + 2t_w d(2t + d)) / 2(tb + 2t_w d) = 19.9 \text{ mm (0.783 in)}$$

$$y_2 = b/2 = 70 \text{ mm (2.756 in)}$$

Moments of Inertia

$$I_1 = b(d+t)^3/3 + d^3(b-2t_w)/3 - A(d+t-y_1)^2 = 2.894 \times 10^5 \text{ mm}^4 (0.695 \text{ in}^4)$$

$$I_2 = (d+t)b^3/12 - d(b-2t_w)^3/12 = 2.110 \times 10^7 \text{ mm}^4 (7.122 \text{ in}^4)$$

The radius of gyration can then be calculated for each axis:

$$r_1 = \sqrt{\frac{I_1}{A}} = 18.7 \text{ mm (0.736 in)}$$

$$r_2 = \sqrt{\frac{I_2}{A}} = 59.7 \text{ mm (2.35 in)}$$

The minimum radius of gyration indicates the weakest orientation for buckling:

$$k = r_1 = 18.7 \text{ mm (0.736 in)}$$

$\ell$ : Length of support plate = 160 mm (6.3 in)

Also, the slenderness ratio,  $\frac{l}{k}$ , is:

$$\frac{l}{k} = \frac{160}{18.7} = 8.6$$

As the ends are fixed, the coefficient “n” becomes 4, so the limit value of the slenderness ratio becomes:

$$85\sqrt{n} = 85\sqrt{4} = 170$$

Because the slenderness ratio of this material is less than the limit value slenderness ratio, Euler's equation is not applicable, and the secant formula for buckling is used. The equation to obtain the support plate's buckling strength is:

$$\frac{P}{A} = \frac{S_y}{1 + \frac{ec}{k^2} \sec \left[ \frac{C\ell}{2k} \sqrt{\frac{P}{AE}} \right]}$$

Where: P: Buckling strength (load) of support column N

A: Area of column = 830.3 mm<sup>2</sup> (1.287 in<sup>2</sup>)

S<sub>y</sub>: Minimum yield strength of Type 304 stainless steel = 206.8 MPa (30.0 ksi)

C: Coefficient to the long support fixed at both ends = 1.2

E: Elastic modulus of Type 304 stainless steel = 1.95 × 10<sup>5</sup> MPa (Table 2-2 at 40°C)

e: Eccentricity small since the strap load is centered = 5 mm (0.2 in)

$\ell$ : Unsupported length of the support column = 160 mm (6.3 in)

c: Shortest distance to an outside side edge from the centroid = 19.9 mm (0.783 in)

Substituting these values in the above equation and solving for P iteratively results in a buckling strength of the support plate column of:

$$P = 1.332 \times 10^5 \text{ N (29,945 lb}_f\text{)}$$

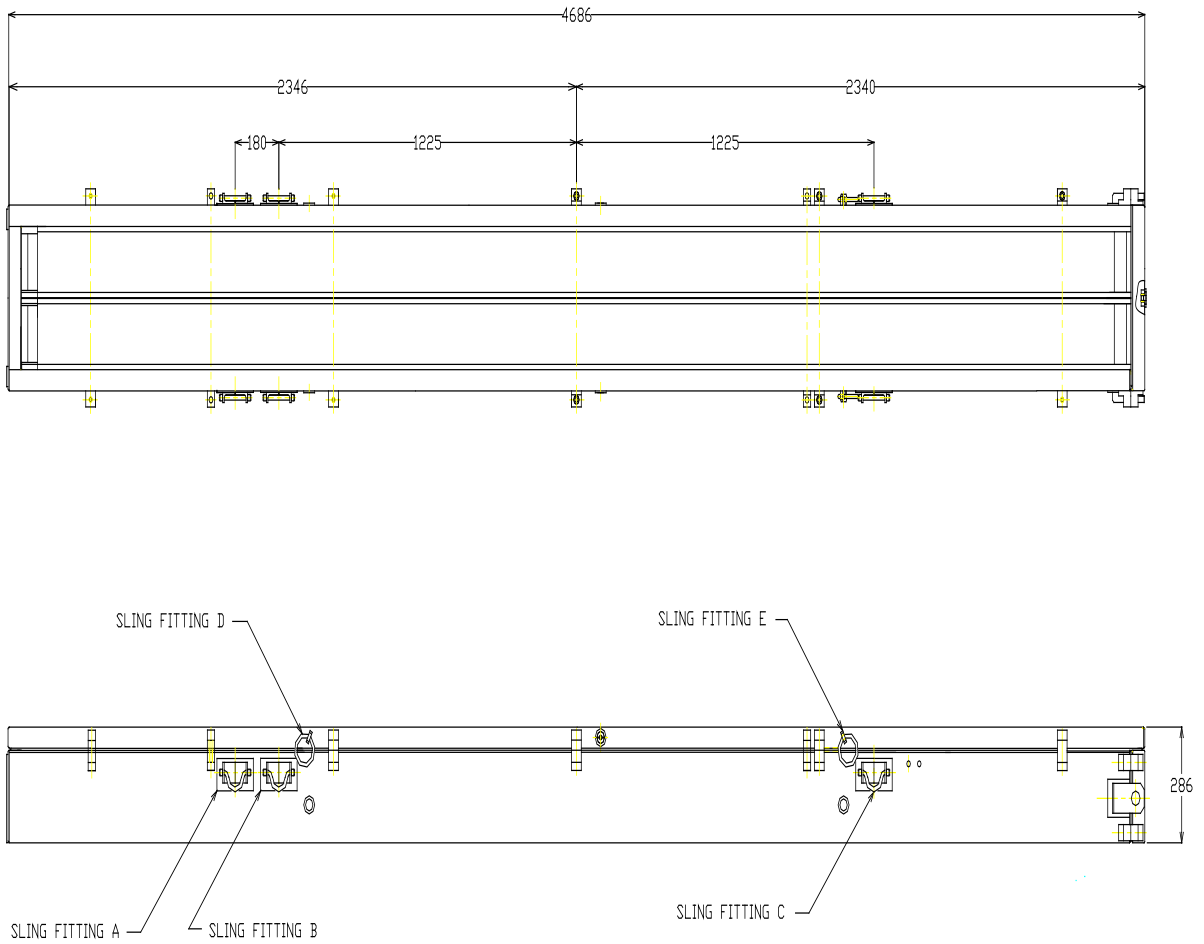
There are four support columns to a side, which results in the sidewall frame having a minimum capacity of:

$$P_t = 4P = 5.328 \times 10^5 \text{ N (119,780 lb}_f\text{)}$$

Since this load capacity is greater than the applied load ( $R_t = 5.259 \times 10^5 \text{ N (1.182} \times 10^5 \text{ lb}_f\text{)}$ ), the supports will not buckle when the worst case tie-down loads are applied to a package. This capacity approaches the force required to yield the columns in compression (i.e.,  $A_{spt}S_y = 6.868 \times 10^5 \text{ N (1.544} \times 10^5 \text{ lb}_f\text{)}$ ).

By considering the stiffening of the support plates with the reinforcement plates used to carry the inner support frame, it has been demonstrated that the support plates have sufficient capacity to react the tie-down load if the package experiences a 5 g lateral and a 2g vertical loading

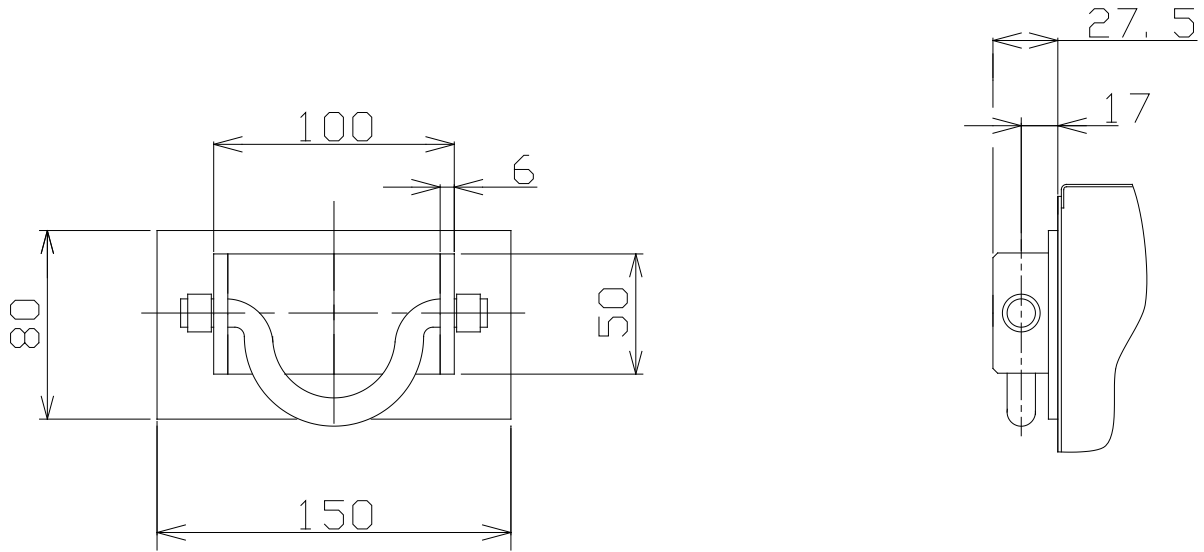
simultaneously. This evaluation does not take into consideration the large carrying capability of the ends of the package where there are corner angles, end plates, and wood overlay plates that further strengthen the package's buckling capability. The use of three or more straps ensures that the load is distributed along the package so that the load can be reacted by the support plates and other internal structure. The stiffness of the OC lid, when the bolster support angles are considered with the reinforced edge of the OC body, ensures that the load is distributed to the internal structure of the package.



(unit: mm)

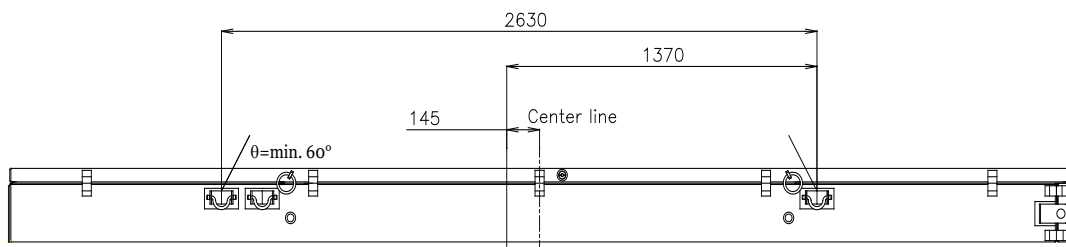
Combination of sling fitting	Used for
A and C	Lifting a Loaded Container
B and C	Lifting an Empty Container
D and E	Lifting a Lid

**Figure 2-2 Inner Container Sling Locations**



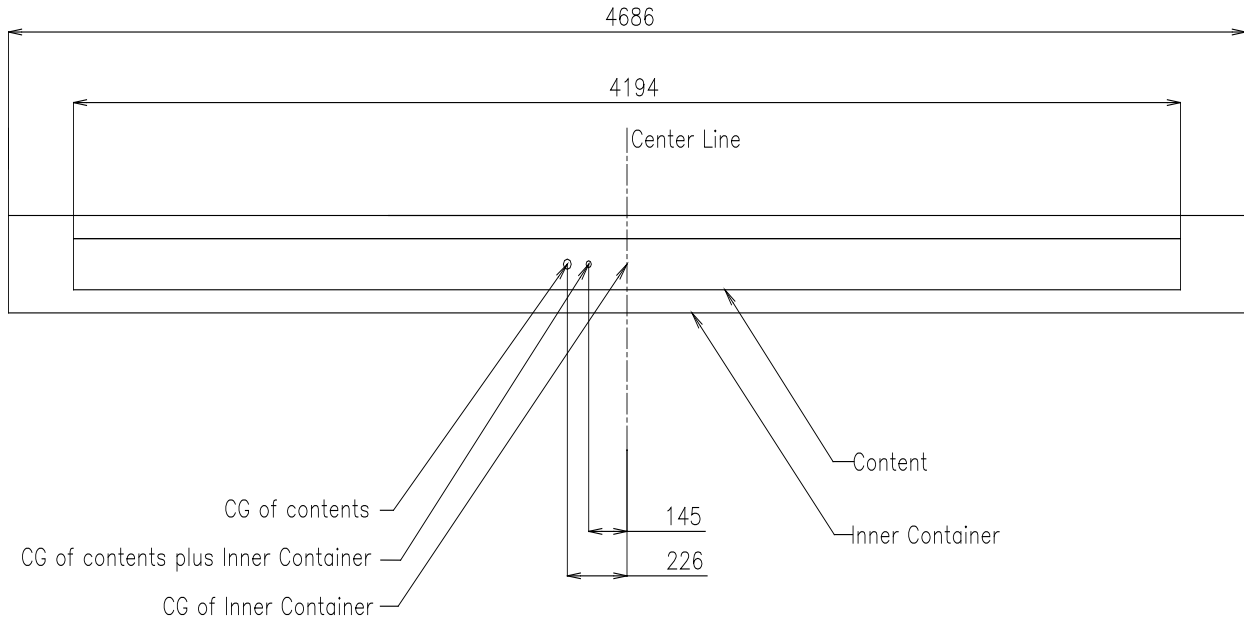
(unit: mm)

**Figure 2-3 Sling Attachment Plate Details**



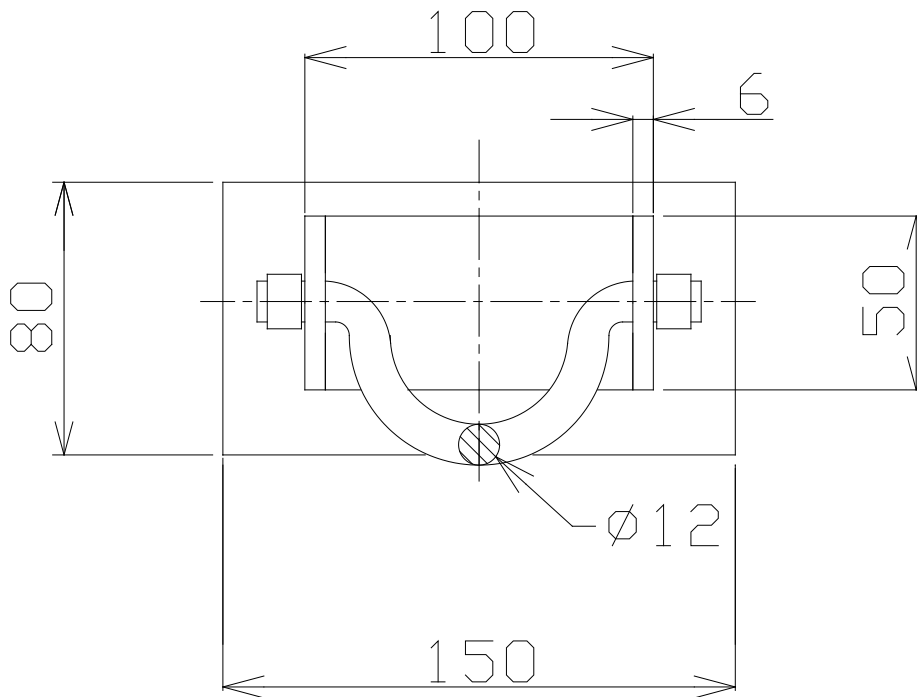
(unit: mm)

**Figure 2-4 Lifting Configuration of Inner Container**



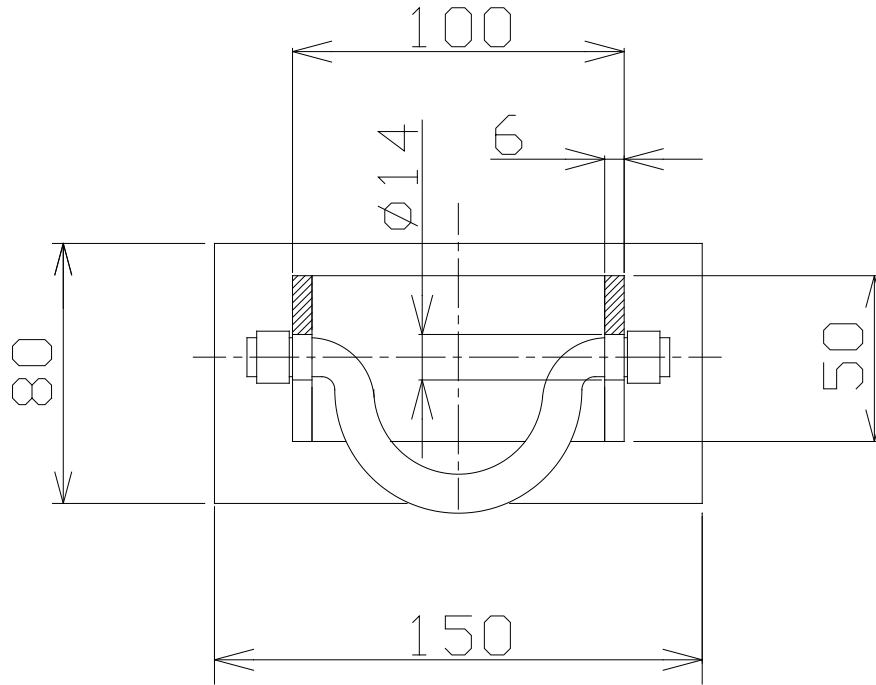
(unit: mm)

**Figure 2-5 Center of Gravity of Loaded Inner Container**



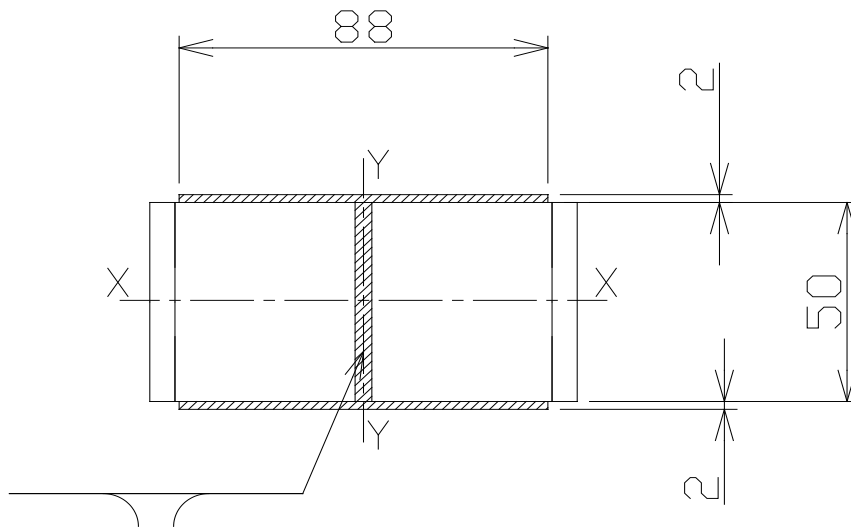
(unit: mm)

**Figure 2-6 Hooking Bar of Sling Fitting**



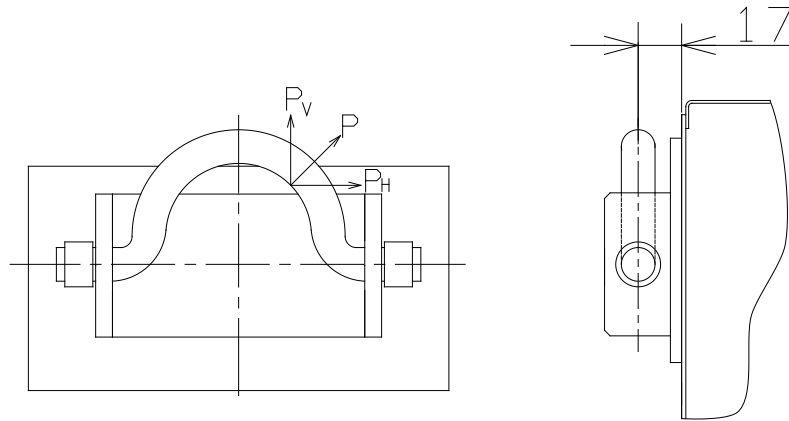
(unit: mm)

**Figure 2-7 Perforated Plate of Sling Fitting**



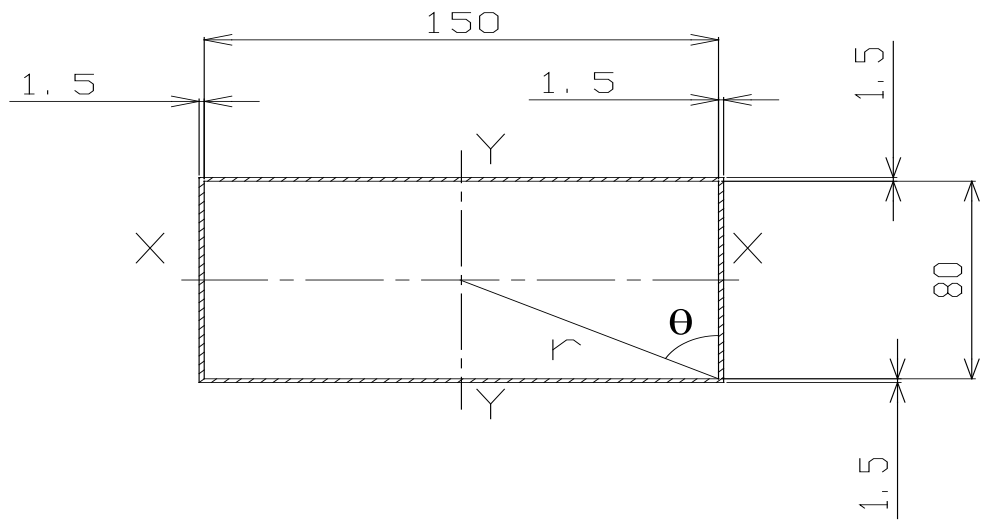
(unit: mm)

**Figure 2-8 Sling Fitting Weld Geometry for Attachment to Support Plate**



(unit: mm)

**Figure 2-9 Loads on Sling Fitting**



(unit: mm)

**Figure 2-10 Welds for Support Plate Attachment to Body**

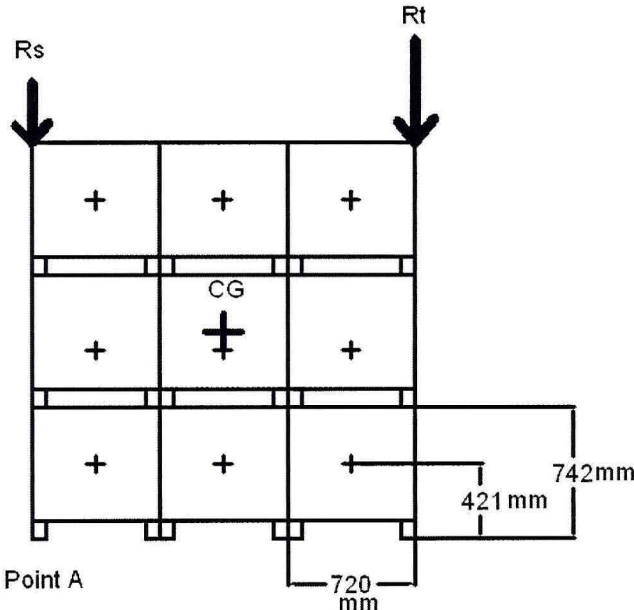


Figure 2-11 Tie-Down Configuration

## **2.5 GENERAL CONSIDERATIONS**

### **2.5.1 Evaluation by Test**

The primary means of demonstrating that the package meets the regulatory accident conditions was by test. The package was tested full-scale by dropping four full-scale certification test units (CTUs) from 9 meters in different orientations. (Two of the test units were dropped as part of the Japanese certification process.) The weight of the units was maximized to provide bounding conditions.

Within the GNF-A CTUs, the fuel was mocked up by a metal boxed section that provided the representative weight in one fuel assembly shipping location. The steel section was segmented to prevent the mockup from adding unrealistic stiffness to the package. In the other fuel assembly shipping position a mock up fuel assembly was used. This had the same cross-sectional properties of the actual fuel. The rods were filled with lead to represent the actual fuel. Weights were added along side of the assembly to provide the correct mass for fuel that may be shipped with channels as well as allowing for the different density between the lead and the uranium oxide pellets.

The units tested in Japan had a simulated 8X8 fuel assembly and weights representing the other fuel assembly in each test unit. The weight and dimensions of the mockup fuel approximated the weight of the fuel to be shipped in the container.

Details of the prototypes used in the drop testing can be found in Section 2.7 and Appendices 2.12.1 and 2.12.2.

The damage caused by the test was evaluated in each of the affected sections, Section 3.0, Section 4.0, and Section 6.0. Both the inner and outer lids stayed in place, although damaged. The inner container holding frame deformed but restrained the inner container. Due to the end drop there was some plastic deformation of the fuel but well within the limits of the criticality evaluation. After the testing, the GNF-A fuel rods passed a helium leakage rate test demonstrating containment.

### **2.5.2 Evaluation by Analysis**

The normal conditions of transport were evaluated by analysis and by comparison to the accident testing. The primary analysis was done for the compression loading. The material properties are taken from Table 2 - 4, which is based on published ASME properties. A static analysis was performed in Section 2.6.9 Compression.

Since the normal condition pressure and temperatures are well below the design conditions for the fuel cladding no separate analysis was performed.

## 2.6 NORMAL CONDITIONS OF TRANSPORT

The RAJ-II package, when subjected to the Normal Conditions of Transport (NCT) specified in 10 CFR 71.71, is shown to meet the performance requirements specified in Subpart E of 10 CFR 71. As discussed in the introduction to this chapter, with the exception of the NCT free drop, the primary proof of NCT performance is via analytic methods. Regulatory Guide 7.6 criteria are demonstrated as acceptable for NCT analytic evaluations presented in this section. Specific discussions regarding brittle fracture and fatigue are presented in Sections 2.1.2.4 and 2.6.5 and are shown not to be limiting cases for the RAJ-II package design. The ability of the welded containment fuel rod cladding to remain leak-tight is documented in Section 4.0.

Properties of Type 304 stainless steel as representative of those properties for 300 series stainless steel are summarized below.

**Table 2 - 5 Material Properties**

Material Property	Material Property Value (psi)			Reference
	-40 °C (-40 °F)	21°C (70 °F)	75°C (167°F)	
<b>Type 304 Stainless Steel</b>				
Elastic Modulus, E	198.6GPa (28.8×10 <sup>6</sup> psi)	195.1GPa (28.3×10 <sup>6</sup> psi)	191.7GPa (27.8×10 <sup>6</sup> psi)	Table 2 - 2
Design Stress Intensity, S <sub>m</sub>	137.9MPa (20,000 psi)	137.9MPa (20,000 psi)	137.9MPa (20,000 psi)	
Yield Strength, S <sub>m</sub>	206.8MPa (30,000psi)	206.8MPa (30,000psi)	184.7MPa (26,788psi)	
Tensile Strength	517.1MPa (75,000psi)	517.1MPa (75,000psi)	498.6MPa (72,300)	

The RAJ-II package's ability to survive HAC, 30-foot free drop, 40-inch puncture drop, and 30-minute thermal event also demonstrated the packages ability to also survive the NCT. Evaluations are performed, when appropriate, to supplement or expand on the available test results. This combination of analytic and test structural evaluations provides an initial configuration for NCT thermal, shielding and criticality performance. In accordance with 10 CFR 71.43(f), the evaluations performed herein successfully demonstrate that under NCT tests the RAJ-II package experiences "no substantial reduction in the effectiveness of the packaging". Summaries of the more significant aspects of the full-scale free drop testing are included in Section 2.6.7, with details presented in Appendix 2.12.1.

## **2.6.1 Heat**

The NCT thermal analyses presented in Section 3.0, consist of exposing the RAJ -II package to direct sunlight and 100 °F still air per the requirements of 10 CFR 71.71(b). Since there is negligible decay heat in the unirradiated fuel, the entire heating came from the solar insolation. The maximum temperature of 77°C (171°F) was located on the lid of the outer container.

### **2.6.1.1 Summary of Pressures and Temperatures**

The fuel assembly exhibits negligible decay heat. The RAJ-II package and internal components, when loaded with the required 10 CFR 71.71(c) (1) insulation conditions, develop a maximum temperature of 77 °C (171 °F). The resulting pressure at the maximum temperature is 1.33 MPa (192.9 psia).

### **2.6.1.2 Differential Thermal Expansion**

With NCT temperatures throughout the packaging being relatively uniform (i.e. no significant temperature gradients), the concern with differential expansions is limited to regions of the RAJ-II packaging that employ adjacent materials with sufficiently different coefficients of thermal expansion. The IC is a double-walled, composite construction of alumina silicate thermal insulator between inner and outer walls of stainless steel. The alumina silicate thermal insulator is loosely packed between the two walls and does not stress the walls. Differential thermal expansion stresses are negligible in the OC for three reasons: 1) the temperature distribution throughout the entire OC is relatively uniform, 2) the OC is fabricated from only one type of structural material, and 3) the OC is not radially or axially constrained within a tight-fitting structure due to the relatively low temperature differentials and lack of internal restraint within the RAJ-II package.

The cladding of the fuel which serves as containment is not stressed due to differential thermal expansion since a gap remains between the fuel pellet and the cladding at both the cold temperature -40°C and the highest temperature the fuel could see due to the HAC which is 800°C. This is demonstrated as follows:

The nominal fuel pellet and cladding dimensions and the resulting radial gap (0.00335 inches) is shown below based on a temperature of 20°C:

As-Built Dimensions (inches)		
Nominal Clad OD	$D_{co}$	0.3957
Nominal Clad ID	$D_{ci}$	0.348
Nominal Pellet OD	$D_{fo}$	0.3413
Nominal Radial Pellet/Clad Gap	$g_n$	0.00335

The strain due to thermal expansion or contraction in the Zr cladding is equal to<sup>a</sup>:

$$\left(\frac{\Delta D}{D}\right)_{clad} = 7.4 \times 10^{-6} (\Delta T)$$

Where  $\Delta T$  is positive for an increase in temperature and negative for a decrease in temperature.

The strain due to thermal expansion or contraction in the fuel pellet is equal to<sup>b</sup>:

$$\left(\frac{\Delta D}{D}\right)_{fuel} = -3.28 \times 10^{-3} + 1.179 \times 10^{-5} T - 2.429 \times 10^{-9} T^2 + 1.219 \times 10^{-12} T^3$$

Where T is the absolute final temperature in degrees Kelvin (K).

The following table summarizes the thermal strain and the thermal growth in the cladding and pellets with a temperature change from 20°C to -40°C ( $\Delta T = -60^\circ C, T = 233K$ ). All dimensions are expressed in inches.

**Table 2 - 6 Thermal Contraction at -40°C**

	Strain at -40°C $\left(\frac{\Delta D}{D}\right)$	Thermal Expansion at -40°C $\left(\frac{\Delta D}{D}\right)D$	Dimension at -40°C $D + \left(\frac{\Delta D}{D}\right)D$
<b>Pellet OD</b>	$-6.49 \times 10^{-4}$	$-2.22 \times 10^{-4}$	0.3411
<b>Cladding ID</b>	$-4.44 \times 10^{-4}$	$-1.55 \times 10^{-4}$	0.3478

This results in a radial gap at -40°C of:

<sup>a</sup> Framatome ANP MOX Material Properties Manual 51-5010288-03

<sup>b</sup> Framatome ANP MOX Material Properties Manual 51-5010288-02

$$g_{-40} = \frac{0.3478 - 0.3411}{2} = 0.0034 \cdot in$$

The following table summarizes the thermal strain and the thermal growth in the cladding and pellets with a temperature change from 20°C to 800°C ( $\Delta T = 780^\circ C, T = 1,073K$ ). All dimensions are expressed in inches.

**Table 2 - 7 Thermal Expansion at 800°C**

	Strain at 800°C $\left(\frac{\Delta D}{D}\right)$	Thermal Expansion at 800°C $\left(\frac{\Delta D}{D}\right)D$	Dimension at 800°C $D + \left(\frac{\Delta D}{D}\right)D$
<b>Pellet OD</b>	$8.08 \times 10^{-3}$	$2.76 \times 10^{-3}$	0.3441
<b>Cladding ID</b>	$5.77 \times 10^{-3}$	$2.01 \times 10^{-3}$	0.3500

This results in a radial gap at 800°C of:

$$g_{800} = \frac{0.3500 - 0.3441}{2} = 0.0030 \cdot in$$

### 2.6.1.3 Stress Calculations

Since the temperatures and pressures generated under normal conditions of transport are well below the design conditions for the boiling water reactor fuel no specific calculations were performed for the fuel containment.

### 2.6.1.4 Comparison with Allowable Stresses

The normal conditions of transport conditions are well below the operating conditions of the fuel no comparison to allowable stresses was performed.

## 2.6.2 Cold

The NCT cold condition consists of exposing the RAJ-II packaging to a steady-state ambient temperature of -40 °F. Insulation and payload internal decay heat are assumed to be zero. These conditions will result in a uniform temperature throughout the package of -40 F. With no internal heat load (i.e., no contents to produce heat), the net pressure differential will only be reduced from the initial conditions at loading.

For the containment, the principal structural concern due to the NCT cold condition is the effect of the differential expansion of the fuel to the zirconium alloy tube. During the cool-down from 20 °C to -40 °C, the tube could shrink onto the fuel because of difference in the thermal expansion coefficient. However, the clearance between the fuel and the cladding is such that even if the fuel did not shrink, there would still be clearance. Differential thermal expansion stresses are negligible in the package for three reasons: 1) the temperature distribution

throughout the entire package is relatively uniform, 2) the package is fabricated from only one type of structural material, and 3) the package is not radially or axially constrained.

Brittle fracture at -40 °F is addressed in Section 2.1.2.4.1.

### **2.6.3 Reduced External Pressure**

The effect of a reduced external pressure of 25 kPa (3.5 psia) per 10 CFR 71.71(c)(3) is negligible for the RAJ-II packaging. The RAJ-II package contains no pressure-tight seal and therefore cannot develop differential pressure. Therefore, the reduced external pressure requirement of 3.5 psia delineated in 10 CFR 71.71(c)(3) will have no effect on the package. Compared with the 1.115 MPa (161.7 psia) internal pressure in the fuel rods, a reduced external pressure of 3.5 psia will have a negligible effect on the fuel rods.

### **2.6.4 Increased External Pressure**

The RAJ-II package contains no pressure-tight seal and, therefore, cannot develop differential pressure. Therefore, the increased external pressure requirement of 140 kPa (20 psia) delineated in 10 CFR 71.71(c)(4) will have no effect on the package. The pressure-tight cladding of the fuel rods is designed for much higher pressures in its normal service in a reactor and is not affected by the slight increase in external pressure.

The containment is provided by the cladding tubes of the fuel. These tubes, designed for the conditions in an operating reactor, have the capability of withstanding the increased external pressure. The failure mode of radial buckling is not a plausible failure mode since the fuel pellets would prevent any significant deformation due to external pressure.

### **2.6.5 Vibration**

The RAJ-II packaging contains an internal shock mount system and, therefore, cannot develop significant vibratory stresses for the package's internal structures. Therefore, vibration normally incident to transportation, as delineated in 10 CFR 71.71(c)(5), will have a negligible effect on the package. Due to concerns of possibly damaging the fuel so it cannot be installed in a reactor after transport, extreme care is taken in packaging the fuel using cushioning material and vibration isolation systems. These systems also ensure that the fuel containment boundary also remains uncompromised. The welded structure of the light weight RAJ-II package is unaffected by vibration. However, after each use the packaging is visually examined for any potential damage.

### **2.6.6 Water Spray**

The materials of construction of the RAJ-II package are such that the water spray test identified in 10 CFR 71.71(c)(6) will have a negligible effect on the package.

### 2.6.7 Free Drop

Since the maximum gross weight of the RAJ-II package is 1,614 kg (3,558 lb), a 1.2 m or four-foot free drop is required per 10 CFR 71.71(c)(7). The Hypothetical Accident Condition (HAC), 9 m (30 foot) free drop test required in 10 CFR 71.73(c)(1) is substantially more damaging than the 1.2 m (4 foot) NCT free drop test. Section 2.7.1 demonstrates the RAJ-II package's survivability and bounds the free drop requirements of 10 CFR 71.71(c)(7). Due to the relatively fragile nature of the fuel assembly payload in maintaining its configuration for operational use, any event that would come close to approximating the NCT free drop would cause the package to be removed from service and re-examined prior to continued use.

As part of the effort to obtain package certification in Japan by GNF-J, certification testing of the package, which included both an end drop and a lid-down horizontal drop, was performed. In each case a 0.3-meter (1-foot) and a 1.2 meter (4-foot) drop was performed prior to the 9-meter (30-foot) drop. In both cases the RAJ-II was slightly damaged but the damage had no significant effect on the performance of the package in relation to either the containment or the ability of the package to meet the requirements of 10 CFR 71. The GNF-J certification testing is discussed in Appendix 2.12.2.

Therefore, the requirements of 10 CFR 71.71(c)(7) are met.

### 2.6.8 Corner Drop

This test does not apply, since the package weight is in excess of 100 kg (220 pounds), and the structural materials used in the RAJ-II are not primarily wood or fiberboard, as delineated in 10 CFR 71.71(c)(8).

### 2.6.9 Compression

Since the package weighs less than 5,000 kg (11,000 pounds), as delineated in 10 CFR 71.71(c)(9), the package must be able to support five times its weight without damage.

The load to be given as the test condition is the load ( $W_1$ ) times five of the weight of this package or the load ( $W_2$ ) which is obtained through multiplying the package's vertical projected area by 13 kPa, whichever is heavier. In the case of this package, the equations to obtain each load are:

$$W_1 = 5 \times m \times g$$

$$W_2 = 13 \text{ kPa} \times L \times B$$

Where:

m: Mass of package	1,614 kg (3,558 lb)
g: Gravitational acceleration	9.81 m/s <sup>2</sup>
L: Length of package	5,068 mm (199.53 in)
B: Width of package	720 mm (28.35 in)

From this

$$W_1 = 5 \times 1,614 \times 9.81 = 79.16 \text{ kN (17,800 lbf)}$$

$$W_2 = 13 \times 10^{-3} \times 5,068 \times 720 = 47.4 \text{ kN (10,660 lbf)}$$

Therefore, as  $W_1 > W_2$ , the stacking load is assumed as  $W = 79.16 \text{ kN (17,800 lbf)}$

The stacking of these packages is as shown in Figure 2-12, so the outer container only sustains the stacking load. In this case, it is assumed that loads are carried by a total of eight support plates positioned in the center of the bolster out of sixteen support plates of the outer container body positioned at the lowest layer. This assumption makes the load sustaining area smaller, so the evaluation is conservative. The compressive load given to the support plate is the above-mentioned stacking load plus the weight of the outer container's lid.

The equation to obtain the support plate's compressive load is:

$$W_c = W_1 + W_3$$

$W_c$ : Compressive load	N
$W_1$ : Stacking load	79.16 kN (17,800 lbf)
$W_3$ : Load by the outer container's lid	1.34 kN (301 lbf)
$m_F$ : Mass of outer container lid	137 kg (302 lb)
g: Gravitational acceleration	9.81m/s <sup>2</sup>

From this, the 80.5 kN (18,100 lbf)

When the fuel assemblies are packed, the gravity center of the outer container is shifted longitudinally, so the load acting on the support plate, which is closer to the gravity center, becomes larger.

Therefore, the equation to obtain the vertical maximum load given to one support plate, which is closer to the gravity center, is:

$$P = \frac{W \cdot \ell_2}{4 \cdot \ell_0}$$

Where:

P: Maximum load acting on one support plate  
 which is nearer to the gravity center N

W: Compressive load given to the support plate 80.5 kN  
 (18,100 lbf)

$\ell_0$ : Longitudinal support plate space 3,510 mm (138.2 in)

$\ell_2$ : Distance from the package's gravity center position  
 to the support

$$\frac{3,510}{2} + 92 = 1,847 \text{ mm (73.76 in)}$$

From this, the maximum load P acted to one support plate, which is nearer to the gravity center, is:

$$P = \frac{80.5 \times 10^3 \times 1,847}{4 \times 3,510} \\ = 10.6 \times 10^3 \text{ N (2,380 lbf)}$$

The resistance of the plate to buckling is also evaluated. The equation to obtain the moment of inertia of area of the support plate which is subject to buckling is:

$$I_z = \frac{1}{12} hb^3$$

Where:

$I_z$ : Moment of inertia of area of support plate mm<sup>4</sup>

b: Thickness of support plate 5 mm (0.2 in)

h: Width of support plate 55 mm (2.2 in)

From this, the moment of inertia of area,  $I_z$ , of the support plate is:

$$I_z = \frac{1}{12} \times 55 \times 5^3 = 572.9 \text{ mm}^4 (1.376 \times 10^{-3} \text{ in}^4)$$

Also, the equation to obtain the radius of gyration of the area of the support plate is:

$$k = \sqrt{\frac{I_z}{A}}$$

Where:

k: Radius of gyration of area of support plate mm

$I_z$ : Moment of inertia of area of support plate 572.9 mm<sup>4</sup> (1.376x10<sup>-3</sup> in<sup>4</sup>)

A: Cross-sectional area of support plate  $5 \times 55 = 275 \text{ mm}^2 (0.426 \text{ in}^2)$

$\ell$ : Length of support plate 559 mm (22.4 in)

From this, the radius of gyration of area k of the support plate is:

$$k = \sqrt{\frac{572.9}{275}} = 1.44 \text{ mm (0.0568 in)}$$

Also, the slenderness ratio  $\frac{\ell}{k}$  is:

$$\frac{\ell}{k} = \frac{559}{1.44} = 388$$

As the ends are fixed, the coefficient n becomes 4, so the limit value of the slenderness ratio becomes as below.

$$85\sqrt{n} = 85\sqrt{4} = 170$$

Because the slenderness ratio of this material, 388, exceeds the limit value of slenderness, Euler's equation is used. The equation to obtain the support plate's buckling strength is:

$$P_k = \frac{n\pi^2 EI_z}{\ell^2}$$

Where:

$P_k$ : Buckling strength (load) of support plate	N
n: Coefficient to the long support fixed at both ends	4
E: Longitudinal elasticity modulus of Gr304 stainless steel	$1.94 \times 10^5$ MPa (at 40°C)
$I_z$ : Moment of inertia of area of support plate	$572.9 \text{ mm}^4$ ( $1.376 \times 10^{-3} \text{ in}^4$ )
$\ell$ : Length of the support plate	559 mm (22.4 in)

From this, the buckling strength  $P_k$  of the support plate is:

$$P_k = \frac{4 \times 3.14^2 \times 1.94 \times 10^5 \times 572.9}{559^2} = 14.0 \times 10^3 \text{ N (3,050)}$$

Therefore,  $P_k > P$ , so the body support plate will not buckle.

### 2.6.10 Penetration

The one-meter (40-inch) drop of a 6 kg (13-pound), hemispherical-headed, 3.2 cm (1.3-inch) diameter, steel cylinder, as delineated in 10 CFR 71.71(c)(10), is of negligible consequence to the RAJ-II package. This is due to the fact that the RAJ-II package is designed to minimize the consequences associated with the much more limiting case of a 40-inch drop of the entire package onto a puncture bar as discussed in Section 2.7.3. The drop of the 6 kg bar will not damage the outer container.

**Table 2 - 8 Temperatures**

<b>Location</b>	<b>Maximum temperature</b>
Environment (Open air)	38°C
Package's external surface	77°C
Inner container	<77°C

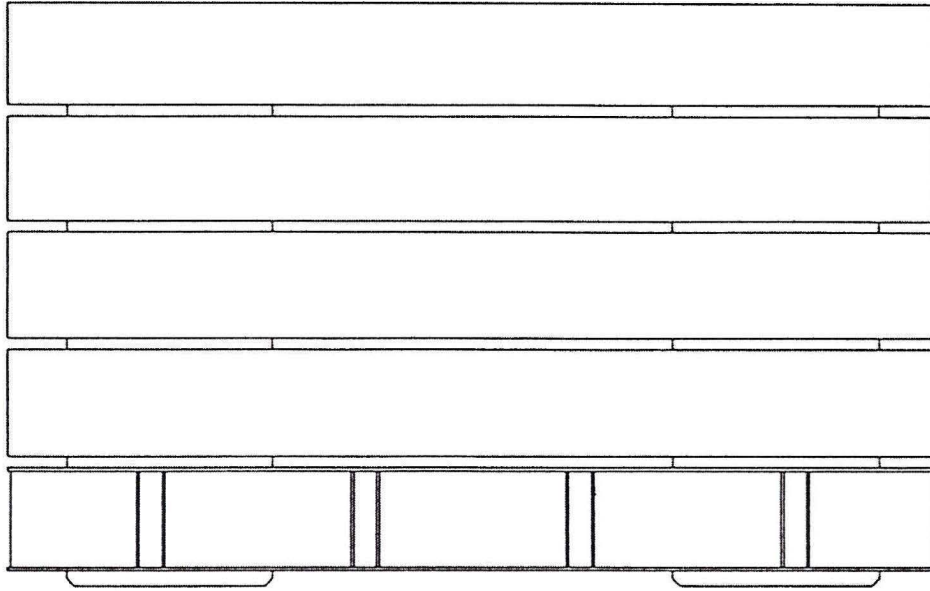


**Figure 2-12 Stacking Arrangement**

## 2.7 HYPOTHETICAL ACCIDENT CONDITIONS

The RAJ-II package, when subjected to the sequence of Hypothetical Accident Condition (HAC) tests specified in 10 CFR 71.73 is shown to meet the performance requirements specified in Subpart E of 10 CFR 71. The primary proof of performance for the HAC tests is via the use of full-scale testing. A certification test unit (CTU) was free dropped, and puncture tested to confirm that both the inner and outer containers protected the fuel and allowed containment to be maintained after a worst-case HAC sequence. Another CTU was free dropped from 9 meters on its end with the fuel maintaining containment after the drop. Observations from CTU testing confirm the conservative nature of the deformed geometry assumptions used in the criticality assessment provided in Chapter 6.0. Immersion is addressed by comparison to the design basis for the fuel.

Test results are summarized in Section 2.7.8, with details provided in Appendix 2.12.1.

### 2.7.1 Free Drop

Subpart F of 10 CFR 71 requires performing a free drop test in accordance with the requirements of 10 CFR 71.73(c)(1). The free drop test involves performing a 30-foot, HAC free drop onto a flat, essentially unyielding, horizontal surface, with the package striking the surface in a position (orientation) for which maximum damage is expected. The ability of the RAJ-II package to adequately withstand this specified free drop condition is demonstrated via testing of four full-scale, certification test units (CTUs).

To properly select a worst-case package orientation for the 30-foot free drop event, items that could potentially compromise containment integrity, shielding integrity, and/or criticality safety of the RAJ-II package must be clearly identified. For the RAJ-II packaging design, there are two primary considerations 1) protect the fuel so that containment is maintained and 2) ensure sufficient structure is around the package to maintain the geometry used in the criticality safety evaluation. Shielding integrity is not a controlling case for the reasons described in Section 5.0. Criticality safety is conservatively evaluated based on measured physical damage to the outer container from certification testing, as described in Section 6.0.

Since the containment is welded closed, the leak-tight capability of the containment may be compromised by two methods: 1) as a result of excessive deformation leading to rupture of the containment boundary, and/or 2) as a result of thermal degradation of the containment material itself in a subsequent fire event and rupture of the weld or the cladding tube by over-pressurization. Importantly, these methods require significant impact damage to the surrounding outer and inner container so that the fuel is either loaded externally or the fuel is directly exposed to the fire.

Additional items for consideration include the possibility of separating the OC lid from the OC body and buckling or deforming of the Outer Container (OC) and/or Inner Container (IC) from an end drop or horizontal drop.

For the above reasons, testing must include impact orientations that affect the lid and stability of the walls of the containers. In general, the energy absorbing capabilities of the RAJ-II are governed by the deformation of the stainless steel and impregnated paper honeycomb that is not significantly affected by temperature.

Appendices 2.12.1 and 2.12.2 provide a comprehensive report of the certification test process and results. Discussions specific to CTU test orientations for free drop and puncture, including initial test conditions, are also provided.

The RAJ-II package has undergone extensive testing during its development. Testing has included 1.2-meter (4-foot) drops on the end in the vertical orientation and the lid in the horizontal orientation. The package has been also dropped from 9 meters in the same orientation demonstrating that the damage from the 1.2-meter (4-foot) drops has little consequence on the performance of the package in 9-meter (30-foot) drop. Based on these preliminary tests it was determined that the worst case orientation for the 9-meter (30-foot) drop test would be slap-down on the lid. The lid down drop demonstrated that the vibration isolation frame bolts would fail allowing the inner container to come in contact with the paper honeycomb in the lid and partially crush the honeycomb. It was expected that the slap-down orientation would maximize the crush of this material minimizing the separation distance between the fuel assemblies in the post accident condition.

A single “worst-case” 9-meter (30-foot) free drop is required by 10 CFR 71.73(c)(1). Based on the above discussion and experience with other long slender packages similar to the RAJ-II, a 15 degree slap-down on the lid was chosen for the 9-meter (30-foot) drop. Following that drop, a 25 degree oblique puncture drop on the damaged lid was performed. See Figure 2-13, Figure 2-14 and Appendix 2.12.1.

Other free drop orientations that were tested include vertical end and bottom corner. These tests demonstrated that the RAJ-II package contains the fuel assemblies without breaching the fuel cladding (containment boundary).

### **2.7.1.1 End Drop**

9-meter (30-foot) end free drops were performed on GNF-J CTU 1J and GNF-A CTU 2. The orientation was selected with the lower end of the fuel down to maximize the damage since the expansion springs in the fuel rods are located in the upper end. This orientation maximized the damage to the energy absorbing wood in the end of the RAJ-II and maximized the axial loading on the fuel assembly. Both tests resulted in deformations of the fuel but were within the limits evaluated in the criticality evaluation in Section 6.0. Following the GNF-A tests, the fuel rods were demonstrated to maintain containment after the free and puncture drops, thus maintaining its containment boundary integrity. Although this orientation caused the most severe damage to the fuel, the damage was well within the structural limits for the fuel and package.

### **2.7.1.2 Side Drop**

No side drop testing was performed in this certification sequence. A side drop test was done in previous testing of the package. That testing resulted in the inner container holding frame top bolts failing and allowing the inner container to come in contact with the outer lid. The inner package showed little damage and the fuel was not deformed. It was judged that the slapdown and the horizontal drop tests bounded the side drop orientation.

### **2.7.1.3 Corner Drop**

A 9-meter (30-foot) free drop on the OC body bottom corner was performed on GNF-J CTU 1J. The impact point previously sustained damage due to 0.3-meter (1-foot) and 1.2-meter (4-foot) free drops. The resultant cumulative deformation was approximately 163 mm (6 inches). There was no loss of contents or significant structural damage to the OC as a result of this free drop. The maximum recorded impact acceleration was 203g. Refer to Appendix 2.12.2 for complete details of the corner free drop.

### **2.7.1.4 Oblique Drops**

An orientation of 15 degrees from horizontal was tested with GNF-A CTU 1. Additional information regarding the selection of this angle is provided in Supplement 1, "Clarifications on the RAJ-II Selection of Slapdown and Puncture Orientations". The IC holding frame was plastically deformed and only a portion of the bolts failed. Neither the fuel nor the IC were not significantly damaged. The damage sustained was bounded by the assumptions utilized in the criticality and thermal evaluations. The fuel was leak tested after the test and was demonstrated to have maintained containment boundary. Refer to Appendix 2.12.1 for complete details of the 15-degree oblique free drop.

### **2.7.1.5 Horizontal Drop**

A 9-meter (30-foot) horizontal free drop on the OC lid was performed on GNF-J CTU 2J. The impact results in a maximum deformation of 19 mm (0.8 inch), which occurred in the OC lid. The side wall of the OC body bulged approximately 19 mm (0.8 inches). Some localized weld failure of OC lid flange/OC lid interface occurred where the bolster angles attach to the lid. None of the OC lid bolts failed as a result of the impact. There was no loss of contents as a result of the free drop. The maximum recorded impact acceleration was 146g. Refer to Appendix 2.12.2 for complete details of the horizontal free drop.

### **2.7.1.6 Summary of Results**

Successful HAC free drop testing of the test units indicates that the various RAJ-II packaging design features are adequately designed to withstand the HAC 30-foot free drop event. The most important result of the testing program was the demonstrated ability of the fuel to remain undamaged and hence maintain its containment capability as defined by ANSI N14.5.

The RAJ-II also maintained its basic geometry required for nuclear criticality safety. Observed permanent deformations of the RAJ-II packaging were less than those assumed for the criticality evaluation.

The GNF-A mock-up fuel assembly rods were leakage rate tested after the conclusion of the testing and were demonstrated to be leaktight, as defined in ANSI N14.5.

A comprehensive summary of free drop test results are provided in Appendices 2.12.1 and 2.12.2.

## **2.7.2 Crush**

Subpart F of 10 CFR 71 requires performing a dynamic crush test in accordance with the requirements of 10 CFR 71.73(c)(2). Since the RAJ-II package weight exceeds 500 kg (1,100 pounds), the dynamic crush test is not required.

## **2.7.3 Puncture**

Subpart F of 10 CFR 71 requires performing a puncture test in accordance with the requirements of 10 CFR 71.73(c)(3). The puncture test involves a 1-meter (40-inch) free drop of a package onto the upper end of a solid, vertical, cylindrical, mild steel bar mounted on an essentially unyielding, horizontal surface. The bar must be 150 mm (6 inches) in diameter, with the top surface horizontal and its edge rounded to a radius of not more than 6 millimeter (0.25 inch). The package is to be oriented in a position for which maximum damage will occur. The length of the bar used was approximately 1.5 meters (60 inches). The ability of the RAJ-II package to adequately withstand this specified puncture drop condition is demonstrated via testing of the full-scale RAJ-II CTUs.

To properly select a worst-case package orientation for the puncture drop event, items that could potentially compromise containment integrity and/or criticality safety of the RAJ-II package must be clearly identified. For the RAJ-II package design, the foremost item to be addressed is the ability of the containment to remain leak-tight. Shielding integrity is not a controlling case for the reasons described in Chapter 5.0. Criticality safety is conservatively evaluated based on measured physical damage to the outer container walls as described in Section 6.0.

Previous testing has shown that the 1-meter drop onto the puncture bar did not penetrate the outer wall or damage the fuel. Based on this previous testing and other experience, an oblique and horizontal puncture drop orientations centered over the fuel were chosen as the most damaging.

Appendices 2.12.1 and 2.12.2 provide a comprehensive report of the certification test process and results. Discussions specific to the configuration and orientation of the test unit are provided.

The “worst-case” puncture drop as required by 10 CFR 71.73(c)(3) was performed on the package with the lid down and 25 degrees from horizontal. The angle was chosen based on experience with other packages and the RAJ-II. Additional information regarding the selection of this angle is provided in Supplement 1, “Clarifications on the RAJ-II Selection of Slapdown and Puncture Orientations”. The puncture bar was aimed at the CG of package to maximize the energy imparted to the package.

The puncture pin did not penetrate the outer container. It deformed the lid inward and it contacted the inner container lid and deformed it a small amount. The outer lid total deformation was less than 12 cm (4.7 inches) and the inner container lid deformed less than 5 cm (2.0 inches).

## **2.7.4 Thermal**

Thermal testing of the GNF-J CTU 2J was performed following the free drop and puncture drop tests (refer to Appendix 2.12.2). Although there was no failure of the containment boundary due to the thermal testing, the thermal evaluation of the RAJ-II package for the HAC heat condition as presented in Section 3.0, demonstrates the regulatory compliance to 10 CFR 71.73(c)(4). Because the RAJ-II package does not contain pressure-tight seals, the HAC pressure for the OC and the IC is zero. The fuel assembly exhibits negligible decay heat.

### **2.7.4.1 Summary of Pressures and Temperatures**

The maximum predicted HAC temperature for the fuel assembly is 921 K (1,198 °F) during the fire event. The fuel rods are designed to withstand a minimum temperature of 1,073 K (1,475 °F) without bursting. This has been demonstrated by heating representative fuel rods to this temperature for over 30 minutes. This heating resulted in rupture pressures in the excess of 3.6 MPa (520 psi). The pressure due to the accident conditions does not exceed 3.5 MPa (508 psig). Summary of pressures and related stresses are provided in Section 3.0.

### **2.7.4.2 Differential Thermal Expansion**

The fuel cladding is not restricted by the packaging and hence can not develop any significant differential thermal expansion stresses. The packaging itself is made of the same metal (austenitic stainless steel) eliminating any significant stresses due to differential thermal expansion.

### **2.7.4.3 Stress Calculations**

Stress calculations for the controlling hoop stress for the fuel cladding that provides containment is provided in Section 3.0.

### **2.7.4.4 Comparison with Allowable Stresses**

The allowable stress used in the analysis in Section 3.0 is based on empirical data from burst tests performed on fuel rods when heated to 800 °C and above. The allowed fuel cladding configurations for the RAJ-II have a positive margin of safety based on stresses required to fail the fuel in the test.

### **2.7.5 Immersion – Fissile Material**

Subpart F of 10 CFR 71 requires performing an immersion test for fissile material packages in accordance with the requirements of 10 CFR 71.73(c)(5). The criticality evaluation presented in Chapter 6.0 assumes optimum hydrogenous moderation of the contents, thereby conservatively addressing the effects and consequences of water in-leakage.

### **2.7.6 Immersion – All Packages**

Subpart F of 10 CFR 71 requires performing an immersion test for packages in accordance with the requirements of 10 CFR 71.73(c)(6). Since the RAJ-II package is not sealed against pressure, there will not be any differential pressure with the water immersion loads defined in 10 CFR 71.73(c)(6). The water immersion will have a negligible effect on the container and the payload, consisting of the fuel assemblies that provide the containment. The fuel rods are designed to withstand differential pressures greater than 1,000 psi. Submergence is a normal design condition for the fuel assemblies and the evaluations are performed on that condition.

### **2.7.7 Deep Water Immersion Test (for Type B Packages Containing More than $10^5$ A<sub>2</sub>)**

Not applicable. The RAJ-II does not contain more than  $10^5$  A<sub>2</sub>.

### **2.7.8 Summary of Damage**

As discussed in the previous sections, the cumulative damaging effects of the free drops and a puncture drop were satisfactorily withstood by the RAJ-II packaging during certification testing. Subsequent helium leak testing confirmed that containment integrity was maintained throughout the test series. The package was also successfully evaluated for maintaining containment during and after the fire event. The deformation of the package in the worst case HAC did not exceed that which is evaluated for in Chapter 6.0. Therefore, the requirements of 10 CFR 71.73 have been satisfied.

**Table 2 - 9 Summary of Tests for RAJ-II**

Test No.	Test Description	Test Unit Angular Orientation		CTU Temperature	Remarks
		Axial <sup>Ⓣ</sup>	Rotational		
1	9 - meter (30-foot) slap down	15°	Lid down	Ambient	Top of package impacted first. Lid crushed over 11 cm (4.3 in).
2	Puncture	25°	Lid down	Ambient	Puncture pin crushed the outer lid down to the inner container lid. It did not rupture the outer lid or significantly deform the inner container lid or fuel.
3	9 - meter (30-foot) end drop	90°	Bottom down	Ambient	Crushed end wood impact absorber. Deformed the fuel assembly but did little damage to the rods

Notes:

- ① Axial angle,  $\theta$ , is relative to horizontal (i.e., side drop orientation)

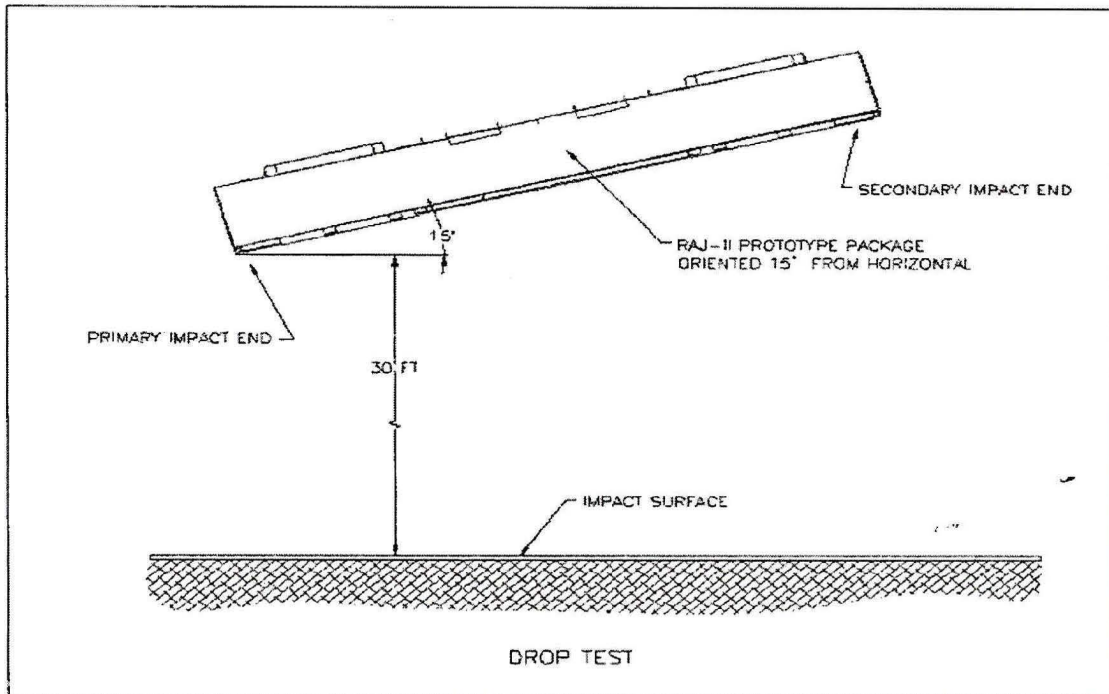


Figure 2-13 Slap-down Orientation

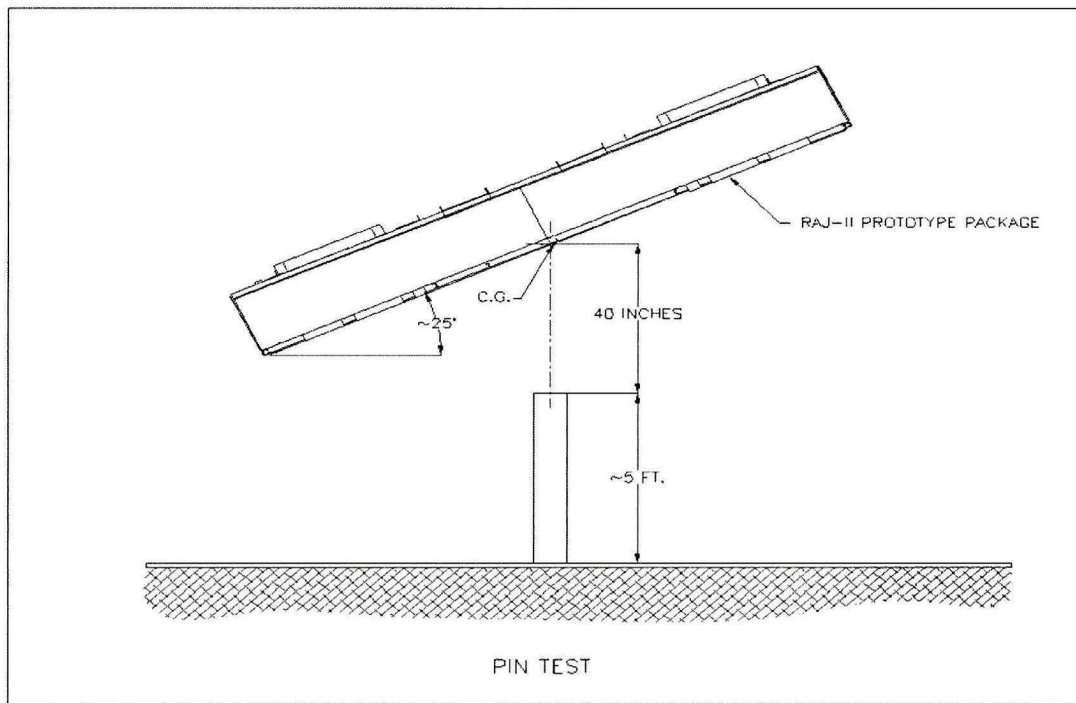
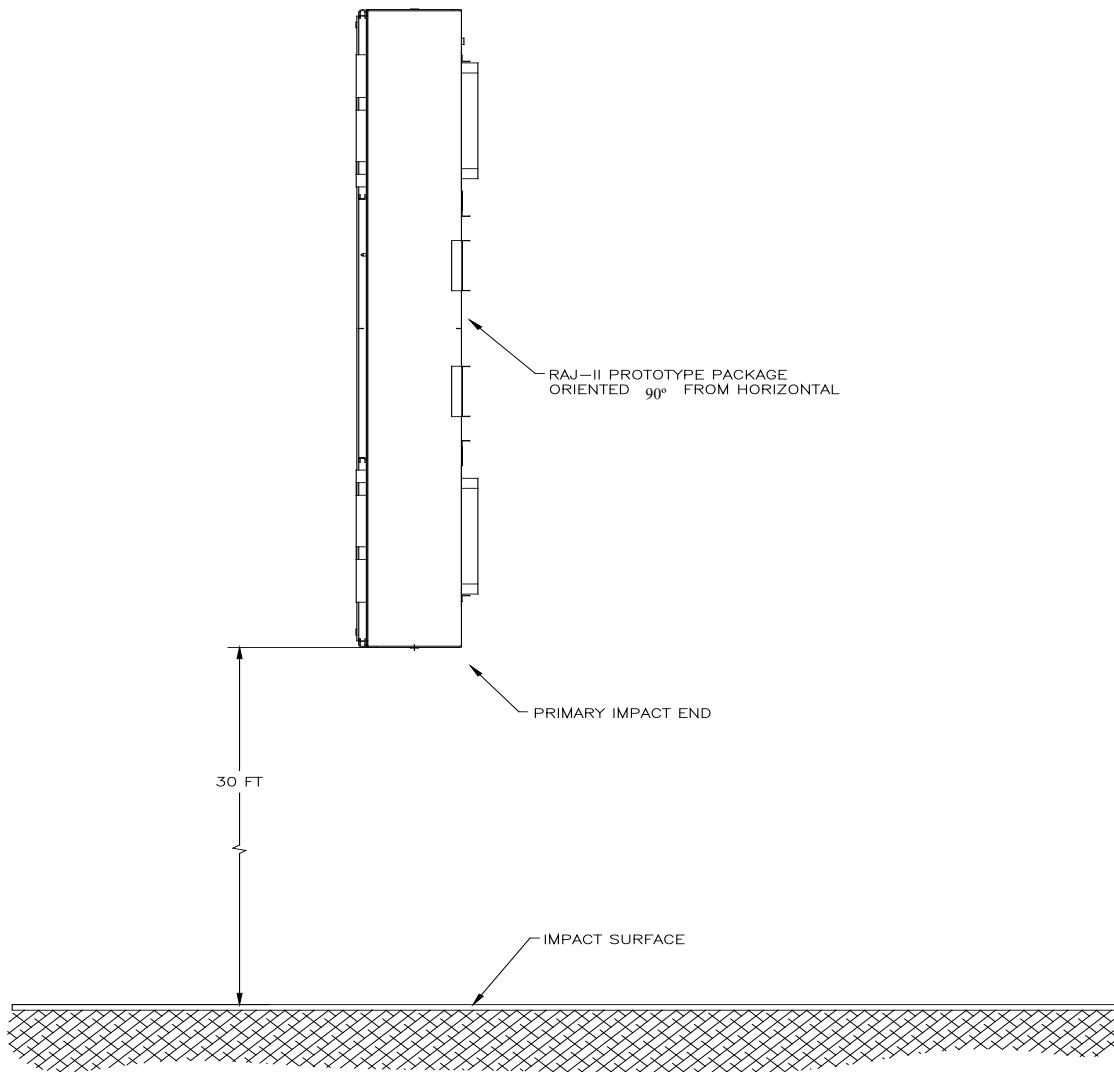


Figure 2-14 Puncture Pin Orientation



**Figure 2-15 End Drop Orientation**

## **2.8 ACCIDENT CONDITIONS FOR AIR TRANSPORT OF PLUTONIUM**

Not Applicable. This package will not be used for the air transport of plutonium.

## **2.9 ACCIDENT CONDITIONS FOR FISSILE MATERIAL PACKAGES FOR AIR TRANSPORT**

Not applicable. This package will not be used for the air transport of fissile material.

## **2.10 SPECIAL FORM**

This section does not apply for the RAJ-II package, since special form is not claimed.

## **2.11 FUEL RODS**

In each event evaluated above either by analysis or by test, the unirradiated fuel rods were protected by the RAJ-II package so that they sustained no significant damage. Fuel rod cladding is considered to provide containment of radioactive material under both normal and accident test conditions. Discussion of this cladding and its ability to maintain sufficient mechanical integrity to provide such containment is described in Section 1.2.3 and Chapter 4.0.

## **2.12 APPENDIX**

### **2.12.1 Certification Tests**

#### **2.12.1.1 Certification Test Unit**

The RAJ-II test packages were fabricated identically to the configuration depicted in the Packaging General Arrangement Drawing found in Appendix 1.4.1. The certification test unit is identical to the production RAJ-II packages except for some minor differences.

1. For ease in documentation/evaluation, tape and marker were used for reference markings during testing.
2. Minor amounts of the internal foam cushioning material were cut out to accommodate added weight in the fuel cavity.
3. Weight was added to the exterior of the package to allow the test units to be at the maximum allowed package weight.

The fuel assemblies were represented by a mock up fuel assembly (an ATRIUM-10 design). Lead rods inside the cladding replaced the fuel pellets. The fuel rods were seal welded using the same techniques used on the production fuel rods. A composite fuel assembly was used to represent the second fuel assembly. Steel tubes represented the ends with added steel for correct weight. The center section was made up of a mock up fuel assembly similar to the full size mock up fuel assembly. The mock up of the fuel approximated the stiffness of the fuel and added no extra strength to the center section of the package that would potentially be damaged by the puncture test. See Figure 2-16 through Figure 2-22 for container and mock up fuel preparation. Weight was added to the fuel assembly cavity by placing lead sheeting on the side of the fuel where normally there is foam. The lead weighing 143 pounds represented the weight of the water channels that could be shipped with some fuel assemblies. The lead plate was cut into strips that were not over half the height of the fuel assemblies to ensure that there was no support or protection added to the fuel during any of the tests. The total weight of the CTUs is provided in Table 2 - 10. The added weight in the contents represents the maximum payload weight including the fuel, fuel assembly fittings and packing material that could be required in the future.

For CTU 1 that was dropped lid down for a 30-foot slap down event and a 1-meter oblique puncture event, the weight was added between the bolster boards at each end. The added weight representing the difference between the actual tare weights of the package and the maximum allowed tare weight consisted of two ½ inch carbon steel plates. For CTU 1, these were held in place by the bolster and brackets attached to the bolster with lag bolts. See Figure 2-23. These plates were taken off CTU 1 and placed on the opposite end of CTU 2 for the end drop. See Figure 2-24.

**Table 2 - 10 Test Unit Weights**

Property	CTU 1		CTU 2	
	kg	lbs	kg	lbs
<b>As fabricated weight</b>	849 kg	1,872 lbs	848 kg	1,869 lbs
<b>Max. fabricated weight</b>	930 kg	2,050 lbs	930 kg	2,050 lbs
<b>Added weight</b>	81.7 kg	180 lbs	81.7 kg	180 lbs
<b>Content weight</b>	684 kg	1,508 lbs	685 kg	1,510 lbs
<b>Measured drop weight</b>	1,614 kg	3,558 lbs	1,611 kg	3,552 lbs
<b>Approximate weight of attaching frame</b>	2.3 kg	5.1 lbs	11.3 kg	24.9 lbs
<b>Approximate drop weight</b>	1,616 kg	3,562 lbs	1,622 kg	3,576 lbs

### **2.12.1.2 Test Orientations**

Three certification tests were performed. Two tests were performed on CTU 1, a 9-meter (30-foot) slap-down on the lid and a 1-meter (40-inch) oblique puncture test on the lid. A 9-meter (30-foot) end drop was performed on CTU 2.

The 9-meter (30-foot) drop on the lid was designed to provide maximum acceleration to the end of the fuel as well as maximize the crush of the package for criticality evaluation purposes. The top down orientation was chosen since the lid contains the least material. The lid down orientation was also chosen since on previous tests horizontal lid down tests had maximized the crush and had resulted in the failure of the retaining bolts on the frame holding the inner container. As discussed in Section 2.7.1.4, the drop orientation was at 15 degrees with the horizontal. See Figure 2-25.

The 1-meter (40-inch) puncture test was performed on CTU 1 with the lid down after the 9-meter (30-foot) slap-down test. The package was oriented at a 25-degree angle to maximize the possibility of the corner of the puncture bar penetrating the outer container and maximizing the damage to the inner container and fuel. The puncture bar was aligned over the center of gravity of the package. See Figure 2-26 and Figure 2-27.

CTU 2 was dropped 9-meters (30-feet) with its bottom end down. The purpose of this orientation was to maximize the damage to the fuel. The bottom end was chosen since it is the most rigid end of the fuel assembly. The expansion springs inside the cladding tubes are on the upper end. See Figure 2-28

### **2.12.1.3 Test Performance**

Testing was performed at the National Transportation Research Center in Oak Ridge, Tennessee. The CTUs were shipped to the facility fully assembled. Only the additional tare weight as described in Section 2.12.1.1 was added at the test facility. Tests were performed on the packages prior to them being transported to the Framatome-ANP facility at Lynchburg, Virginia. At Lynchburg the packages were disassembled and examined and the fuel rods were helium leak tested.

The slapdown test at 15 degrees to horizontal demonstrated the ability of the outer package to protect the fuel and the inner container. The energy absorbing capabilities of the package allowed the package to deform and limited the secondary impact to less than the primary impact. See Figure 2-29 and Figure 2-30. This test resulted in deformation inside the package. See Figure 2-36 and Figure 2-37. The crush of the paper honeycomb was limited by the stiffening plates in the lid. See Figure 2-38. The inner container lid was deformed as well. Neither the lid bolts on either container nor the bolts on the inner container clamping device failed. The frame did bend over 3 cm. The fuel rods, although slightly deformed due to the test and the added weight in the fuel cavity, were not damaged. See Figure 2-39. The added weight placed between the bolster timbers caused a slight deformation of the bottom wall of the outer package in the local area of the weights.

The puncture test was performed with the lid down at a 25 degree angle from horizontal. See Figure 2.26 and 2.27. The puncture pin was bolted with three bolts to the drop pad. The puncture pin struck the lid over the CG of the package after the package had undergone the slapdown test. The pin did not penetrate the outer lid. The outer lid was deformed inward until it came in contact with the inner container. This was confirmed by a slight mark on the inner container lid. The pin appears to have bounced since there are two indentations very close together which could have been caused by the outer lid bottoming out against the inner container lid. See Figure 2-31 and Figure 2-32. No significant internal package or fuel damage appeared to be attributable to the pin puncture test.

The 9-meter (30-foot) end drop test was performed on CTU 2 with the bottom end down. There was little exterior damage to the outer container. See Figure 2-33, Figure 2-34, and Figure 2-35. Extensive damage occurred to the inside of the inner container as the fuel assemblies and the added weight impacted the interior of the inner container. The rigid end fitting of the assembly crushed the wood located at the end of the package. Although some welds broke, the bottom end of the package remained in place. The fuel rods partially came out of the end fitting. The fuel assemblies bent to the side. See Figure 2-40, Figure 2-41, and, Figure 2-42.

The mock up fuel assemblies from both CTU 1 and CTU 2 were helium leak tested. The Assembly from CTU 1 was found to meet the leak tight requirements of having a leak rate less than  $1 \times 10^{-7}$  atm-cc/s. The assembly from CTU 2 was found to have a He leak rate of  $5.5 \times 10^{-6}$  atm-cc/s. This is within the allowable leakage for the fuel as shown in Section 4.0.

#### **2.12.1.4 Test Summaries**

Two 9-meter (30-foot) drops and one oblique puncture pin test were performed on two certification test units. The packages retained the fuel assemblies and protected the fuel. Mockup fuel assemblies from both certification units were leak tested after the drop tests and were determined to have maintained containment. The tests are summarized below.

**Table 2 - 11 Testing Summary**

Test	CTU	Orientation with horizontal	Exterior damage	Interior damage	Fuel
9-meter (30-foot) lid down	1	15°	Minor deformation on both ends.	No bolts broken on the frame or the lids. Significant deformation to inner container and internal clamp frame. Reduction of spacing between outside of package and fuel to about 4 inches.	Minimal damage to the fuel assemblies. Some twist to the assembly. No real damage to the fuel rods. The fuel was demonstrated to have a leak rate of less than $1 \times 10^{-7}$ atm-cc/s after the testing.
1-meter (40 in) lid down over cg	1	25°	Did not penetrate outer wall	Outer wall contacted inner container. Section 2.12 Figure 2-39 through 2-42 show some damage to the inner container, however, this damage is conservatively modeled in the HAC criticality analyses in Section 6.0 and is not sufficient to allow fuel to leak from the container.	The fuel appeared not to be affected by this test. Passed helium leak test.
9-meter (30-foot) lower end	2	90°	Localized damage on impact end.	Major crushing of the wood at the end of the inner package and breaking of the inner wall of the inner container on the impacted end. The outer wall was damaged but did not fail completely.	Fuel was bent and separated from end fittings. Fuel spacers were damaged. Fuel rods had no significant damage. Fuel bending was influenced by the movement of the weight added to the fuel cavity. Post drop leak test giving a He leak rate of $5.5 \times 10^{-6}$ atm-cc/s demonstrated that containment had been maintained.



**Figure 2-16 Inner Container Being Prepared to Receive Mockup Fuel and Added Weight**

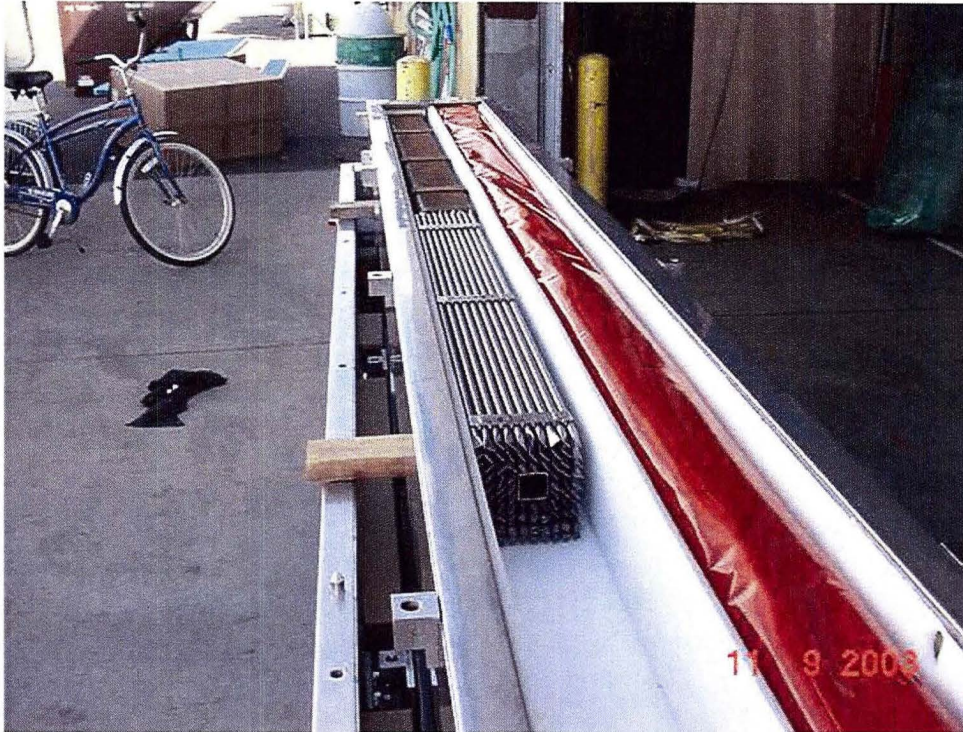


**Figure 2-17 Partial Fuel Assemblies in CTU 1**



**Figure 2-18 Top End Fittings on Fuel in CTU 1**

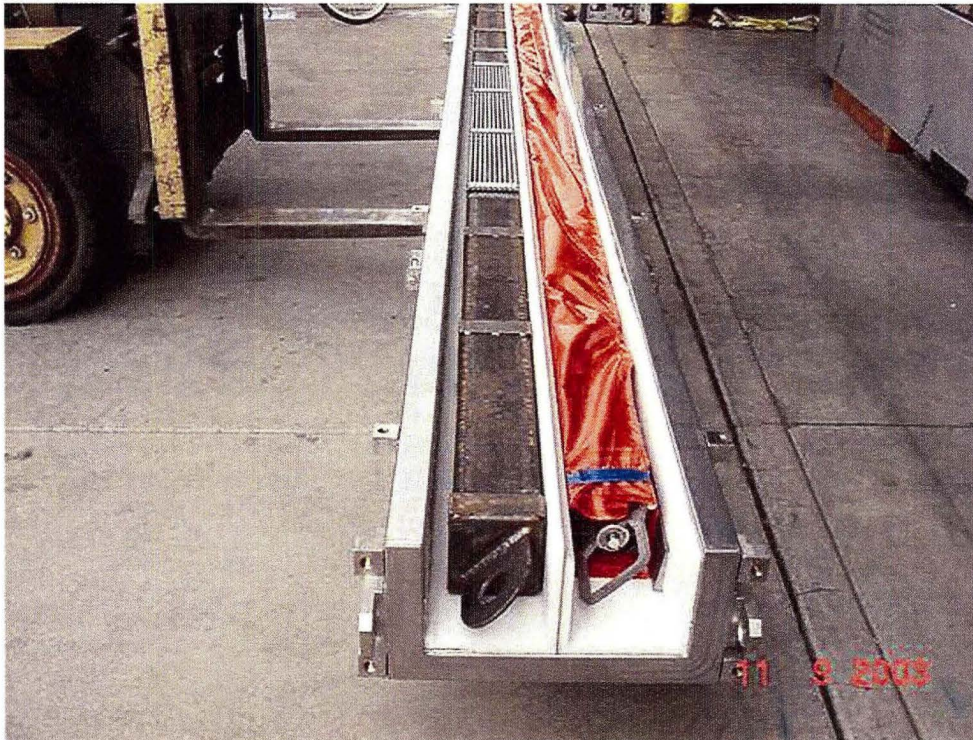


**Figure 2-19 Contents of CTU 2**



**Figure 2-20 Outer Container without Inner Container**



**Figure 2-21 Inner Container Secured in Outer Container**

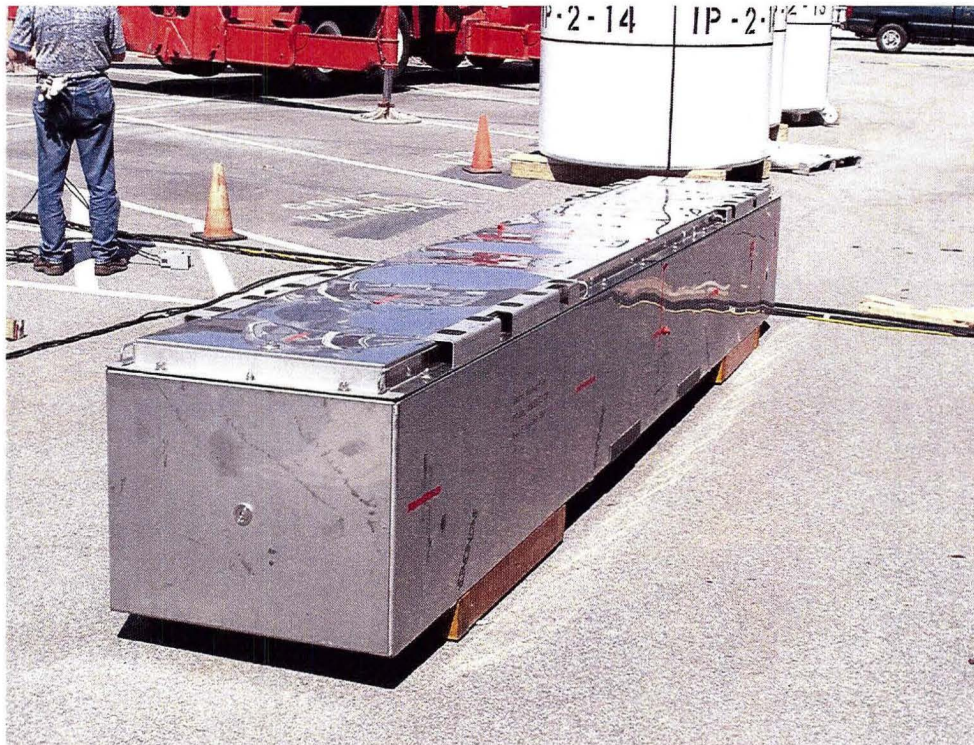


**Figure 2-22 CTU 2 Prior to Testing**



**Figure 2-23 Addition of Tare Weight to CTU 1**



**Figure 2-24 Addition of Tare Weight to CTU 2**



**Figure 2-25 CTU 1 Positioned for 15° 9-m (30-foot) Slap-down Drop**



**Figure 2-26 Alignment for Oblique Puncture**



**Figure 2-27 Position for Puncture Test**



**Figure 2-28 Position for End Drop**



**Figure 2-29 Primary Impact End Slap-down Damage**



**Figure 2-30 Secondary Impact End Damage**



**Figure 2-31 Puncture Damage**



**Figure 2-32 Close Up of Puncture Damage**



**Figure 2-33 End Impact**